

CHD1 remodelers regulate nucleosome spacing *in vitro* and align nucleosomal arrays over gene coding regions in *S. pombe*

Since Advance Online Publication, accession codes have been added.

Julia Pointner^{1,3}, Jenna Persson^{2,3},
Punit Prasad^{2,3}, Ulrika Norman-Axelsson²,
Annelie Strålfors², Olga Khorosjutina²,
Nils Krietenstein¹, J Peter Svensson²,
Karl Ekwall^{2,4,*} and Philipp Korber^{1,4,*}

¹Adolf-Butenandt-Institut, University of Munich, Munich, Germany and
²Department of Biosciences and Nutrition, Karolinska Institutet, Center
for Biotechnology, Huddinge, Sweden

Nucleosome positioning governs access to eukaryotic genomes. Many genes show a stereotypic organisation at their 5' end: a nucleosome free region just upstream of the transcription start site (TSS) followed by a regular nucleosomal array over the coding region. The determinants for this pattern are unclear, but nucleosome remodelers are likely critical. Here we study the role of remodelers in global nucleosome positioning in *S. pombe* and the corresponding changes in expression. We find a striking evolutionary shift in remodeler usage between budding and fission yeast. The *S. pombe* RSC complex does not seem to be involved in nucleosome positioning, despite its prominent role in *S. cerevisiae*. While *S. pombe* lacks ISWI-type remodelers, it has two CHD1-type ATPases, Hrp1 and Hrp3. We demonstrate nucleosome spacing activity for Hrp1 and Hrp3 *in vitro*, and that together they are essential for linking regular genic arrays to most TSSs *in vivo*. Impaired arrays in the absence of either or both remodelers may lead to increased cryptic antisense transcription, but overall gene expression levels are only mildly affected.

The EMBO Journal (2012) 31, 4388–4403. doi:10.1038/emboj.2012.289; Published online 26 October 2012

Subject Categories: chromatin & transcription

Keywords: antisense transcription; CHD1; nucleosome positioning; remodeling; *S. pombe*

Introduction

DNA-templated processes, like transcription and replication, are central to cellular life. However, DNA access is encumbered in eukaryotes as nuclear DNA is packaged into protein-nucleic acid structures collectively called chromatin. The basic chromatin units are nucleosomes (Kornberg, 1974; Kornberg and Lorch, 1999), where ~147 bp are wound in ~1.7 turns around a histone protein octamer (Davey *et al*, 2002; Richmond and Davey, 2003), and variable lengths of linker DNA connect such nucleosome core particles. Nucleosome core particle DNA is generally less accessible for DNA binding factors than free DNA (Bell *et al*, 2011). Indeed, there is a plethora of cofactors for DNA-templated processes that deal with the (re-)organisation of chromatin, for example, histone modifying enzymes (Kouzarides, 2007; Henikoff and Shilatifard, 2011), histone variants (Bonisch and Hake, 2012), and nucleosome remodeling enzymes (Clapier and Cairns, 2009). The latter are of particular importance as all regulation through chromatin boils down to the question of whether a certain region of DNA is occluded by nucleosomes or not. It is the remodeling enzymes that render nucleosomes dynamic, i.e., remodel, slide, space, dis- and reassemble nucleosomes or exchange histones.

Therefore, understanding genome regulation through chromatin is primarily a question of understanding the mechanisms of nucleosome positioning. Where are nucleosomes relative to the DNA sequence? What places them or removes them from there? Recently, the first question received abundant answers as nucleosomes were mapped genome-wide in many species (Yuan *et al*, 2005; Mavrich *et al*, 2008; Valouev *et al*, 2008; Lantermann *et al*, 2010; Valouev *et al*, 2011). This revealed that a major portion of nucleosomes indeed adopts well-defined positions, especially in regions that are important for regulation, like promoters and replication origins (Jiang and Pugh, 2009; Radman-Livaja and Rando, 2010; Iyer, 2012). Particularly at gene starts there is often a stereotypic organization with a broad (~150–200 bp) nucleosome free region (NFR) just upstream of the transcription start site (TSS) that is flanked by highly positioned nucleosomes (+1, sometimes also –1 nucleosome). The +1 nucleosome is usually the first of an array of regularly spaced nucleosomes extending into the gene body. Sometimes arrays also form upstream of the NFR. As this NFR-array organization comprises the majority of positioned nucleosomes, the mechanism(s) leading to it will answer the bulk of the second question above.

Regarding the generation of NFRs, specific DNA binding proteins may compete away the histone octamer and prevent nucleosome formation. Indeed, there is ample evidence that specific binders, like Reb1 and Abf1 in budding yeast (Raisner

*Corresponding authors. K Ekwall, Department of Biosciences and Nutrition, Karolinska Institutet, Center for Biotechnology, Huddinge, Sweden. Tel.: +46 85 2481039; Fax: +46 87745538;

E-mail: Karl.Ekwall@ki.se or P Korber, Adolf-Butenandt-Institut, University of Munich, Schillerstr. 44, Munich 80336, Germany.

Tel.: +49 89 218075435; Fax: +49 89 218075425;

E-mail: pkorber@lmu.de

³These authors contributed equally to the work.

⁴Shared last authors.

Received: 23 July 2012; accepted: 28 September 2012; published online: 26 October 2012; corrected: 28 November 2012

et al, 2005; Hartley and Madhani, 2009; Bai *et al*, 2011) or CTCF in mammals (Fu *et al*, 2008), contribute to NFR generation. Further, there is a clear role for intrinsic DNA features that translate into DNA sequence dependent histone octamer binding preferences. For example, poly(dA:dT) (Iyer and Struhl, 1995; Sekinger *et al*, 2005; Segal *et al*, 2006; Kaplan *et al*, 2009; Segal and Widom, 2009) or poly(dG:dC) (Tsankov *et al*, 2011) disfavour, and 10 bp periodicities of certain dinucleotides (Satchwell and Travers, 1989; Segal *et al*, 2006; Brogaard *et al*, 2012) favor the tightly bent DNA path for nucleosome formation. Interestingly, a genome-wide comparison of 13 ascomycetes yeasts revealed species-specific preferences for nucleosome positioning mechanisms (Tsankov *et al*, 2010; Tsankov *et al*, 2011). For the same class of genes, some yeasts rely on poly(dA:dT) elements for NFR formation, some on poly(dA:dT) plus Abf1, some only on Abf1, or for a different class some yeasts replace Reb1 with Cbf1. Very recently, different mechanisms for NFR formation at replication origins in fission yeasts were found (Xu *et al*, 2012). While *S. pombe* and *S. octosporus* employ poly(dA:dT) elements, *S. japonicus* uses poly(dG:dC), the Reb1-homolog Sap1 and an unknown CTCGTC-binding factor.

In contrast to explanations for NFR generation, we only poorly understand what positions the +1 nucleosome and what generates the regular arrays. The so far prevailing 'statistical positioning' model (Kornberg and Stryer, 1988; Mobius and Gerland, 2010), which could elegantly explain array formation by passive statistical movement of nucleosomes against a fixed barrier, was recently called into question. The model predicts that the average spacing of nucleosomes within arrays depends on nucleosome density. However, constant spacing despite lower nucleosome density was observed both *in vitro* (Zhang *et al*, 2011) and *in vivo* (Celona *et al*, 2011; Gossett and Lieb, 2012). Therefore, an active packing mechanism was proposed where ATP dependent activities align nucleosomes with constant spacing at the +1 nucleosome/NFR/TSS (Zhang *et al*, 2011).

Remodeling enzymes are the best candidates for such packing activities. They are all DNA translocases and belong to the Snf2-subfamily of helicases, which is further divided into subtypes like the SWI/SNF-, ISWI- and CHD-types (Flaus *et al*, 2006). They all remodel nucleosome structure, but their association with other subunits and their exact mechanisms, regulation, recruitment and products differ. Indeed, there is initial evidence for specific roles of specific remodelers in nucleosome positioning, especially in *S. cerevisiae*. The RSC remodeling complex has a specific role in the generation of NFRs and positioning of the flanking nucleosomes in budding yeast (Parnell *et al*, 2008; Badis *et al*, 2008; Hartley and Madhani, 2009; Wippo *et al*, 2011). The Isw1 and Isw2 remodelers help to position nucleosomes in the middle of genes or flanking the NFR, respectively (Whitehouse *et al*, 2007; Tirosch *et al*, 2010; Yen *et al*, 2012). The absence of Isw1 and Chd1 dramatically impaired array formation (Gkikopoulos *et al*, 2011). Finally, specific remodelers were shown to associate with specific nucleosome positions (Yen *et al*, 2012). Now we need evolutionary comparisons in order to assess how conserved these mechanisms are.

The fission yeast *S. pombe* is becoming increasingly popular as model for chromatin biology. Its far divergence from budding yeast (~1 billion years (Heckman *et al*, 2001)) allows powerful evolutionary comparisons and many

aspects of its chromatin biology, e.g., centromere and heterochromatin structure (Ekwall, 2007; Grewal, 2010), are more similar to metazoans than those of budding yeast. We published the first genome-wide nucleosome map in *S. pombe* (Lantermann *et al*, 2010), which was confirmed by two other groups recently (Tsankov *et al*, 2011; Givens *et al*, 2012). This map showed important differences in nucleosome organization between *S. pombe* and *S. cerevisiae*, which was also followed up by others (Tsankov *et al*, 2011). For example, *S. pombe* has no enrichment of poly(dA:dT) elements at promoter NFRs and shows much less pronounced arrays upstream of the NFR (Lantermann *et al*, 2010), but does use the Reb1-homolog Sap1 for NFR formation (Tsankov *et al*, 2011).

Here we report on the role of remodeling enzymes in nucleosome positioning in *S. pombe*. We find that the CHD1-type remodelers Hrp1 and Hrp3 are responsible for generating the TSS-aligned genic nucleosomal arrays throughout the genome. We show for the first time that Hrp1 and Hrp3 have nucleosome spacing activity *in vitro*, and their absence *in vivo* can, but need not, lead to gene expression changes including upregulation of cryptic antisense transcription. Surprisingly, the role of RSC in nucleosome positioning, even though very prominent in *S. cerevisiae*, seems not to be conserved in *S. pombe*.

Results

Neither the histone variant H2A.Z nor the remodeling enzyme Swr1 has a major role in nucleosome positioning

H2A.Z is the major variant of histone H2A (Bonisch and Hake, 2012), present in most species, and the only H2A variant in *S. pombe* (encoded by *pht1*) and *S. cerevisiae* (encoded by *HTZ1*). In both yeasts, the remodeling ATPase Swr1 is specifically required to deposit H2A.Z in exchange for H2A (Mizuguchi *et al*, 2004; Buchanan *et al*, 2009). Interestingly, H2A.Z is often enriched in both nucleosomes flanking promoter NFRs in *S. cerevisiae* (Raisner *et al*, 2005), while it resides mainly in the +1 and less in the -1 nucleosome of *S. pombe* (Buchanan *et al*, 2009). The enrichment of H2A.Z in the best positioned nucleosomes suggested a role of this histone variant in nucleosome positioning. However, in budding yeast NFR formation was necessary for H2A.Z deposition, but not the other way around, ruling out a causal role for H2A.Z in nucleosome positioning (Hartley and Madhani, 2009). Nonetheless, a possible role of H2A.Z in nucleosome positioning also had to be tested for *S. pombe*. Importantly, phenotypes of mutants lacking H2A.Z can also be due to the effects of Swr1 in the absence of its natural substrate (Halley *et al*, 2010). It is therefore mandatory to use a double mutant deleted for the genes encoding H2A.Z and Swr1.

We constructed a *pht1Δ swr1Δ* double deletion mutant and measured genome-wide nucleosome occupancy by hybridizing MNase generated mononucleosomal DNA fragments to Affymetrix tiling arrays. A TSS-aligned nucleosome occupancy composite plot for all genes did not show much of a difference from the wild-type (wt) pattern, with a slight effect on +1 nucleosome occupancy (Figure 1A). As effects on a subset of genes may not be visible in such composite plots, we specifically looked at loci where a function of H2A.Z may

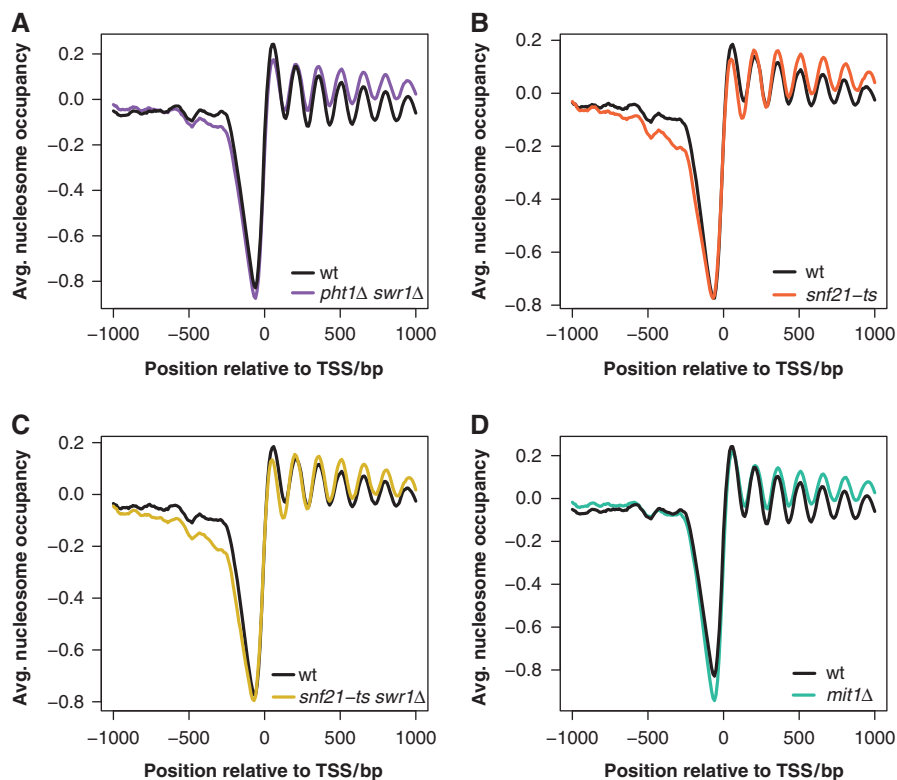


Figure 1 H2A.Z, Swr1, Snf21 and Mit1 do not have a major role in nucleosome positioning around TSSs in *S. pombe*. Overlay of TSS-aligned nucleosome occupancy profiles for 4013 genes in (A) wt (Hu303, average of five biological replicates) and *pht1Δ swr1Δ* (Hu2127, average of two biological replicates) at 30°C, (B) wt (K240/Hu2261, average of two biological replicates) and *snf21-ts* (KYP176/Hu2262, average of two biological replicates) after 6 h at 34°C, (C) wt (as in (B)) and *snf21-ts swr1Δ* (Hu2314, average of two biological replicates) after 6 h at 34°C, and (D) wt (as in (A)) and *mit1Δ* (Hu1294, average of two biological replicates) at 30°C.

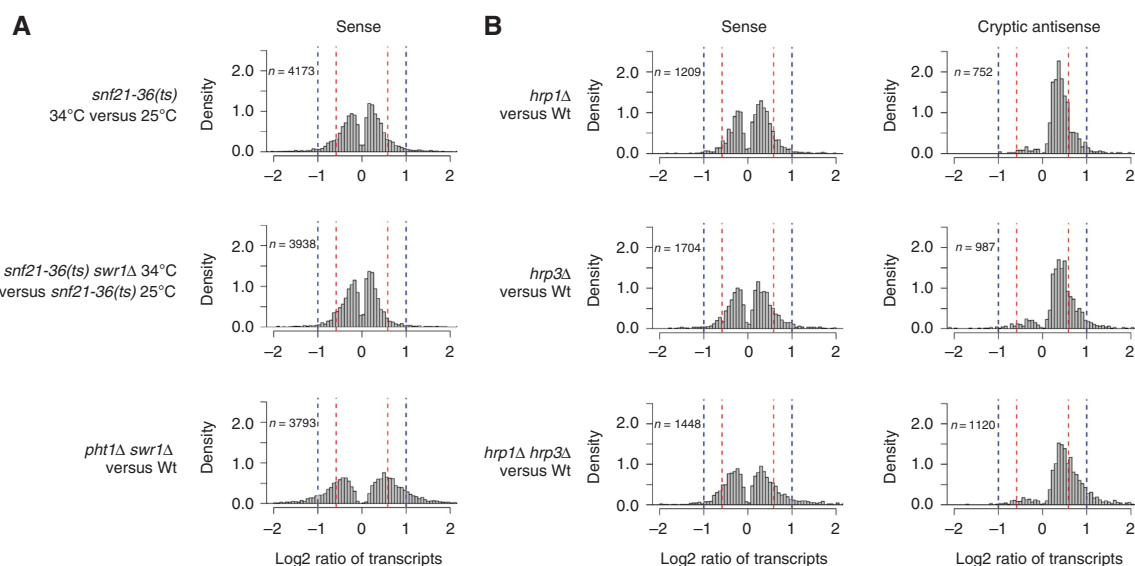


Figure 2 Histogram of transcript level changes as summarized in Table I. (A) Sense transcript levels of the indicated mutants relative to respective controls. (B) Sense and cryptic antisense transcript levels relative to wt for the indicated mutants. Red and blue dashed lines depict the 1.5 fold and 2 fold thresholds, respectively. The total number of changed transcripts (n) is indicated in the upper left corner of each panel.

be expected. First, we distinguished targets from non-targets in terms of H2A.Z binding (ChIP-chip data of (Buchanan *et al*, 2009)) (Supplementary Figure 1A). Second, we distinguished responders from non-responders in terms of changed expression levels in the double mutant compared to wt, of which there were many (Table I, Figure 2A and Supplementary

Figure 1B and C). Nonetheless, neither subgroup showed much of an effect on the mutant nucleosome occupancy patterns arguing against a major role of H2A.Z or Swr1 in global nucleosome positioning in fission yeast. Further, neither transcriptome responder subgroup overlapped much with the H2A.Z targets speaking either for not exhaustive

ChIP-chip data or for indirect effects (Supplementary Figure 1D).

As noted before (Lantermann *et al*, 2010), the H2A.Z binding genes showed more pronounced -1 to -3 nucleosomes in the composite plot and a shoulder at the $3'$ flank of the -1 nucleosomes amounting to a much more narrow promoter NFR (Supplementary Figure 1A). This special nucleosome pattern is not caused by H2A.Z or Swr1 as it was unchanged in the absence of both.

The RSC remodeling complex does not seem to be involved in nucleosome positioning around TSSs

The RSC remodeling complex is the only remodeling enzyme essential for viability, both in *S. cerevisiae* (ATPase subunit encoded by *STH1*, (Cairns *et al*, 1996)) and in *S. pombe* (ATPase encoded by *snf21* (Yamada *et al*, 2008)). Conditional ablation of RSC activity in *S. cerevisiae* led to increased nucleosome occupancy in a majority of NFRs (Parnell *et al*, 2008; Badis *et al*, 2008; Hartley and Madhani, 2009). Given the high conservation of its essential requirement and of the RSC core complex composition (Monahan *et al*, 2008), we guessed that RSC's function in NFR formation was also highly conserved, and wished to test it in *S. pombe*.

We obtained a temperature sensitive *snf21-ts* *S. pombe* mutant (Yamada *et al*, 2008) and determined the restrictive conditions such that cells stopped growing, but were still viable. After six hours incubation at 34°C *snf21-ts* cells stopped growing as measured by cell number (Supplementary Figure 2A), but were mostly still alive as only $<3\%$ of cells were pink in phloxin B vital dye staining assay. Viability as judged by colony formation after plating at 25°C was somewhat lower (Supplementary Figure 2A), which reflected that resumption of cell division is a more stringent assay for viability than active pumping of phloxin B out of cells. In addition to the phenotypes of growth arrest and imminent cell death, we also observed pronounced elongation of cell shape (Supplementary Figure 2B) as well as substantial changes in the transcriptome (Table I, Figure 2A).

Despite this clear induction of a phenotype at these restrictive conditions, we did not observe substantial changes in the composite nucleosome occupancy profile, besides slight effects on occupancy in the -1 and $+1$ nucleosome region (Figure 1B). The effects were not exacerbated if transcriptome responder subgroups were considered (Supplementary Figure 3A and B).

We even combined the *snf21-ts* and *swr1 Δ* mutations, but the nucleosome profile of this *snf21-ts swr1 Δ* double mutant very much mirrored that of the *snf21-ts* single mutant (Figure 1C). Also here the subgroups of transcriptome responders did not show stronger effects (Supplementary Figure 3C and D).

Collectively and counter to expectation, the RSC nucleosome remodeling complex does not seem not to be much involved in nucleosome positioning around TSSs in *S. pombe*.

The previously described role of the Mit1 remodeling ATPase in genic array formation could not be reproduced with improved technology

A triple deletion of both ISWI-type remodeling ATPases (Isw1 and Isw2) and the one CHD-type ATPase (Chd1) present in *S. cerevisiae* virtually abolished the appearance of regular genic arrays in composite TSS-aligned nucleosome occu-

pancy plots (Gkikopoulos *et al*, 2011). The *S. pombe* genome does not encode any ISWI-, but three CHD-type remodeling ATPases: Hrp1, Hrp3 of the CHD1-type and Mit1 of the Mi-2-type (Flaus *et al*, 2006). The Mit1 ATPase is part of the SHREC complex that was implicated in nucleosome positioning at the heterochromatic mating type locus (Sugiyama *et al*, 2007). Previously, we observed less pronounced genic arrays in a *mit1 Δ* mutant (Lantermann *et al*, 2010). Since then we have improved our methodology (see Materials and methods) such that a consistently more even fragmentation of the mononucleosomal DNA prior to hybridization is achieved. In the course of testing *S. pombe* mutants lacking various remodeling enzymes, we also revisited the *mit1 Δ* mutant with this improved methodology and could not detect any substantial difference from the wt (Figure 1D), not even for the subgroup of transcriptome responders (Supplementary Figure 4). We now conclude that Mit1 does not play a major role in nucleosome positioning in *S. pombe* euchromatin around TSSs. Apparently, uneven fragment size distributions of the three biological replicates used before (Lantermann *et al*, 2010) led to the observed less regular nucleosome pattern. This highlights the importance of hybridizing homogeneously fragmented mononucleosomal DNA to Affymetrix tiling arrays.

Lack of Hrp1 and Hrp3 remodeling enzymes dramatically compromises the formation of regular genic arrays downstream of the $+2$ nucleosome

As the absence of Mit1 did not show much of an effect anymore, we turned to the other two CHD1-type remodelers Hrp1 and Hrp3. An *hrp1 Δ* mutant had a mild effect on the amplitude of the genic arrays, especially toward the $3'$ end (Figure 3A). This effect was more pronounced in the *hrp3 Δ* mutant (Figure 3B). Strikingly, the combined absence of Hrp1 and Hrp3 completely blurred the nucleosome occupancy peaks downstream of the $+2$ position (Figure 3C). Importantly, the $+1$ and $+2$ nucleosome peaks were not affected in position but only in occupancy, especially the $+2$ nucleosome. We tried to generate an *hrp1 Δ hrp3 Δ mit1 Δ* triple mutant, but obtained no viable cells. In order to validate the Affymetrix array data we analyzed three loci in wt, *hrp1 Δ* , *hrp3 Δ* and *hrp1 Δ hrp3 Δ* cells by indirect end labeling (Supplementary Figure 5). There was not much difference between the wt and *hrp1 Δ* MNase pattern, but there were clear differences between wt and the *hrp3 Δ* or *hrp1 Δ hrp3 Δ* mutants consistent with our genome-wide data. As noted before (Mason and Mellor, 1997; Lantermann *et al*, 2009; Givens *et al*, 2011), there was a rather strong endogenous nuclease activity in *S. pombe* chromatin preparations as detected by mock MNase digestions (Supplementary Figure 6). This endogenous nuclease pattern background encumbers clear assignments of MNase patterns but does not compromise the conclusions about MNase pattern differences between wt and mutants.

The impairment of TSS-aligned genic arrays was also reflected in spectral analyses of the nucleosome occupancy data, which reveal periodic nucleosome positioning patterns relative to genomic coordinates (Lantermann *et al*, 2010). The broad peak around two nucleosomes per 1000 bp corresponds to low frequency noise, but the more pointed peak around 6.5 nucleosomes per 1000 bp reflects the average nucleosome repeat length (NRL). This latter peak was well visible for wt, less clear and a bit shifted towards slightly

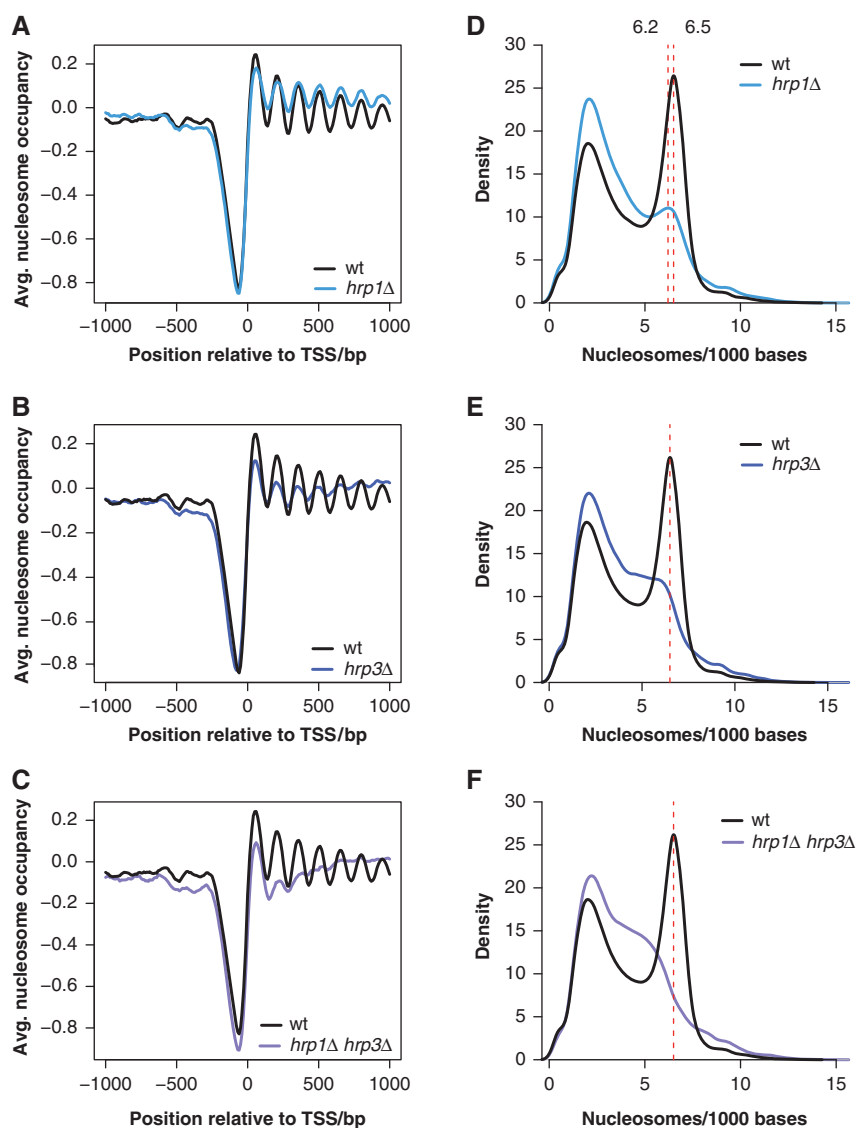


Figure 3 Hrp1 and Hrp3 together are critical for the generation of TSS-aligned genic nucleosome arrays. Overlay of TSS-aligned nucleosome occupancy profiles for 4013 genes in wt (Hu303, average of five biological replicates), (A) *hrp1*Δ (Hu2239, average of two biological replicates), (B) *hrp3*Δ (Hu0575/EJY321, average of two biological replicates) and (C) *hrp1*Δ *hrp3*Δ (Hu2303, average two biological replicates) at 30°C. (D–F) Spectral analysis as in (Lantermann *et al*, 2010) for the data in panels (A–C), respectively. 6.2 or 6.5 nucleosomes per 1000 bp translate into a NRL of 161 or 154 bp in *hrp1*Δ or wt, respectively.

wider spacing for the *hrp1*Δ mutant and progressively turned into a shoulder of the broad noise peak for the *hrp3*Δ and *hrp1*Δ *hrp3*Δ mutants (Figure 3D–F). We conclude that nucleosome positioning patterns over coding regions are progressively compromised in the absence of Hrp1, Hrp3 and both together.

We also checked whether subgroups of genes, either targets in terms of Hrp1 and/or Hrp3 binding (combined ChIP-chip data for IGR and ORF of each remodeler as published in (Walfridsson *et al*, 2007)) or transcriptome responders in terms of changed expression levels compared to wt (Table I, Figure 2B), revealed more or very different changes in nucleosome occupancy profiles in these mutants relative to the patterns of the non-targets or relative to the same subgroups for the wt. Indeed, Hrp3 binding targets showed even more pronounced defects in genic arrays in both the *hrp3*Δ and the *hrp1*Δ *hrp3*Δ mutants (Figure 4A and B). At these targets the +2 and the downstream nucleosomes were more

affected, i.e., there was hardly any peak modulation in the pattern anymore. This argues for a direct effect of Hrp3 on nucleosome organisation. This increased effect was not really visible for Hrp1 binding targets (Supplementary Figure 7A and B), but also these targets were still clearly affected in the *hrp1*Δ *hrp3*Δ mutant. Even genes that were not measured to bind either Hrp1 or Hrp3 also had compromised genic arrays in the *hrp1*Δ *hrp3*Δ mutant (Supplementary Figure 7C). This rather loose correlation between remodeler binding targets and chromatin change responders may either speak for indirect effects or for nonexhaustive measurement of remodeler binding by ChIP. We favor the latter in light of the notorious difficulties detecting remodeling enzymes by ChIP (e.g., Gelbart *et al*, 2005). Just recently a study failed to ChIP Chd1 over coding regions in *S. cerevisiae* with a more stringent MNase-ChIP-seq protocol (Yen *et al*, 2012) even though it was detected at single loci by classical ChIP before (Simic *et al*, 2003). Interestingly, Hrp1 and Hrp3

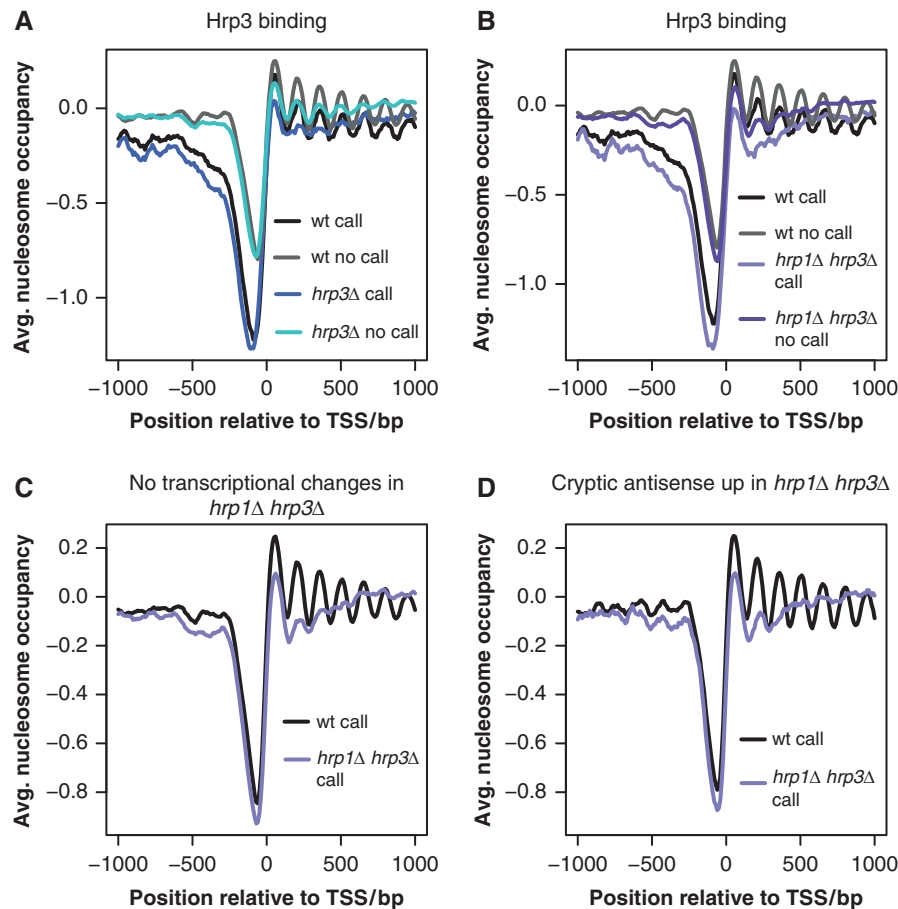


Figure 4 Effects on genic arrays are stronger for Hrp3-bound loci, also seen for genes without substantially changed expression levels in the *hrp1Δ hrp3Δ* mutant, and not stronger for loci with increased cryptic antisense transcription. (A) and (B) Data as in Figure 3B and C, respectively, but divided into Hrp3-bound (369 calls) and -unbound (3644) loci (Walfridsson *et al*, 2007). (C) Data as in Figure 3C, but only genes without any transcriptional changes (2570 calls). (D) Data as in Figure 3C, but only genes with upregulated cryptic antisense transcription (828 calls).

targets both had a broader NFR in wt, which was not caused by these enzymes as it was still present in the *hrp1Δ hrp3Δ* mutant (Figure 4B and Supplementary Figure 7B). We wonder if such extended regions of free DNA serve as preferred recruitment sites for Hrp1 and Hrp3.

The up- or downregulated genes in the *hrp1Δ*, *hrp3Δ* or *hrp1Δ hrp3Δ* mutants did not show increased effects relative to the non-responders in the mutant or relative to the same subgroup in the wt (Supplementary Figure 8A-F). Similar to the loose correlation with Hrp1 and Hrp3 binding targets, a change in chromatin structure did not necessarily correlate with changes in expression. This was especially striking in the case of the *hrp1Δ hrp3Δ* double mutant where even the subgroup of non-responders still showed the same impaired nucleosome pattern (Figure 4C). This argues against a strict causal relationship between changes in chromatin structure and changes in expression level, very much as seen before in *S. cerevisiae* for the *isw1 isw2 chd1* mutant (Gkikopoulos *et al*, 2011), and against changes in transcription levels as the cause of changes in chromatin.

Transcriptome changes in hrp mutants included upregulation of cryptic antisense transcripts

As impaired genic arrays are linked to increased cryptic transcription in *S. cerevisiae* (Cheung *et al*, 2008; Quan

and Hartzog, 2010; Owen-Hughes and Gkikopoulos, 2012; Radman-Livaja *et al*, 2012; Smolle *et al*, 2012) we included actinomycin D in the reverse transcriptase reaction for expression analysis of the *hrp1Δ*, *hrp3Δ* and *hrp1Δ hrp3Δ* mutants in order to accurately quantitate antisense transcription (Perocchi *et al*, 2007). Indeed, both single mutants and even more so the double mutant showed increased cryptic antisense transcription, i.e., transcripts that are antisense to an annotated genomic element, but not annotated themselves (Table I, Figure 2B). We also checked whether intergenic regions lacking annotated transcripts became more transcribed in the *hrp* mutants. However, this was not the case.

We wondered whether changes in cryptic antisense transcription affected the respective sense transcripts, but the correlation is negligible (Supplementary Figure 9). As deletion of *hrp1* leads to defects in transcription termination (Alen *et al*, 2002), we tested whether responders with increased cryptic antisense transcription were enriched for genes with convergent orientation or whether responders with increased sense transcription were enriched for the downstream genes of tandem gene pairs. The latter was not the case (*P*-values of 0.48, 0.10 and 0.09 for the *hrp1Δ*, *hrp3Δ* and *hrp1Δ hrp3Δ* mutants, respectively; Fisher's exact test), and only the *hrp1Δ hrp3Δ* mutant showed a significant

enrichment of the former kind (*P*-values of 0.042, 0.058 and 0.006 for the the *hrp1Δ*, *hrp3Δ* and *hrp1Δ hrp3Δ* mutants, respectively; Fisher's exact test). The convergent genes with upregulated cryptic antisense transcription did show a somewhat different nucleosome occupancy profile in the double mutant as the +3 to +5 nucleosome peaks were more pronounced compared to the rather flat pattern usually seen in this double mutant (Supplementary Figure 10A). Nonetheless, the effect was slight and we do not emphasize it. In general, loci with increased cryptic antisense transcription did not show increased or different effects on nucleosome positioning (Figure 4D). We conclude that termination defects do not explain the majority of increased cryptic antisense transcription, and that impaired genic arrays can but need not cause increased cryptic antisense transcription.

We also asked the reverse question of whether a mutant with increased cryptic transcription, like a *set2* deletion mutant (Zofall *et al*, 2009), showed impaired nucleosome organization. However this was not true (Supplementary Figure 10B), not even for genes enriched in the modification product of Set2, H3K36Me (Supplementary Figure 10C), arguing against cryptic transcription causing compromised arrays.

Deletion of *hrp1* and/or *hrp3* did not abolish regular spacing of bulk nucleosomes as monitored by MNase ladders

One might expect that mutants with impaired genic arrays would also show impaired regular spacing of bulk nucleosomes. However, limited MNase digestion of chromatin from the *hrp1Δ*, *hrp3Δ* and *hrp1Δ hrp3Δ* mutants and unspecific bulk detection of DNA fragments by ethidium bromide (MNase ladder assay) did not show pronounced differences from wt (Supplementary Figure 11A). This argues that Hrp1 and Hrp3 are not necessary for regular spacing of nucleosomes as such, but for linking regular arrays to the reference point of the NFR/+1 nucleosome (see Discussion).

Bulk MNase ladders were also still detectable in an *isw1 isw2 chd1* triple mutant in *S. cerevisiae*

The defect in the TSS-aligned nucleosome occupancy composite profile of the *hrp1Δ hrp3Δ* mutant (Figure 3C) was strikingly similar to that in an *isw1 chd1* double or *isw1 isw2 chd1* triple mutant in *S. cerevisiae* (Gkikopoulos *et al*, 2011). We wondered whether bulk MNase ladders were not much affected in the latter *S. cerevisiae* mutants, either. Gkikopoulos *et al* (2011) observed less clear MNase ladders in the *isw1 chd1* and *isw1 isw2 chd1* *S. cerevisiae* mutants. However, these effects were somewhat subtle and not reported in an earlier chromatin study that used mutants deleted in the same genes (Tsukiyama *et al*, 1999). We revisited this issue and performed bulk MNase ladder assays using either the exact same *isw1 isw2 chd1* triple mutant from J Mellor as used by Gkikopoulos *et al* or the triple mutant generated by T Tsukiyama in a different strain background (Tsukiyama *et al*, 1999). We reproduced a compromised appearance of MNase ladders in Mellor's strain (Supplementary Figure 11B). This was especially true regarding signal intensity, which may argue for increased overall nuclease sensitivity, i.e. fewer canonical nucleosomes. However, we detected much less difference in Tsukiyama's strain (Supplementary Figure 11C), reminiscent

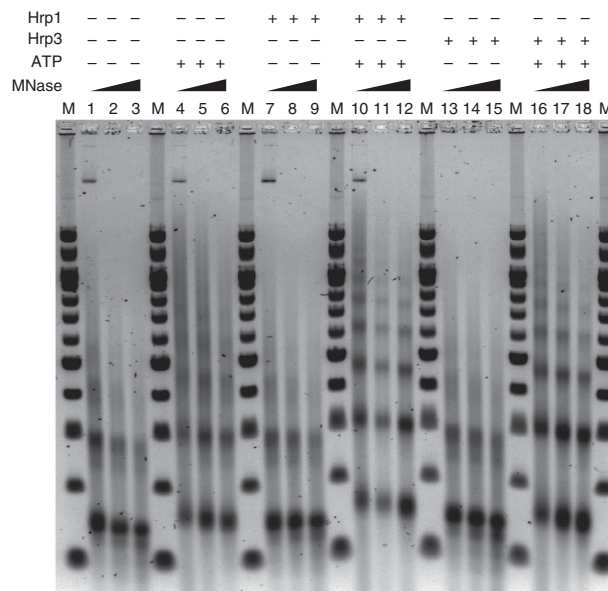


Figure 5 Hrp1 and Hrp3 efficiently space nucleosomes *in vitro* in an ATP-dependent manner. Phage λ DNA salt dialysis chromatin was incubated with Hrp1, Hrp3 and ATP as indicated above the lanes and digested with MNase. Wedges on top of the lanes correspond to increasing concentrations of 1, 2 and 4 U/ml. 'M' denotes 100 bp marker (New England Biolabs).

of the *S. pombe hrp1Δ hrp3Δ* mutant. While the differences between Mellor's and Tsukiyama's triple mutants may be attributed to differences in strain background, it is clear for both *S. cerevisiae* mutants that regular bulk nucleosome spacing was not entirely lost.

Hrp1 and Hrp3 have nucleosome spacing activity *in vitro*

CHD1 in *D. melanogaster* was demonstrated to have nucleosome spacing activity *in vitro* (Lusser *et al*, 2005), and Chd1 of *S. cerevisiae* preferentially moves nucleosomes to a center position on short DNA templates (Stockdale *et al*, 2006), which is indicative of generating regular spacing in arrays. Even though Hrp1 and Hrp3 proteins are CHD1 homologs, their remodeling activities have thus far not been demonstrated and characterised *in vitro*. So it was important to confirm by direct measurement that a role in nucleosome spacing *in vivo* corresponded to the respective activity *in vitro*. We purified FLAG-tagged Hrp1 and TAP-tagged Hrp3 from *S. pombe* and analyzed the preparations by mass spectrometry, alongside of samples of respective mock purifications (Supplementary Figure 12A, Supplementary Table I). Hrp1 and Hrp3 copurified with a few proteins unspecifically as these were also present in the respective mock purifications. Most notably, Hrp1 bound unspecifically to FLAG M2 agarose beads and Hrp3 copurified specifically with all four canonical histones (Supplementary Figure 12A, Supplementary Table I).

To assemble chromatin templates *in vitro*, we constructed vectors for the expression of the recombinant canonical *S. pombe* histones in *E. coli*, purified the histones and refolded them into octamers. Phage lambda DNA was reconstituted into chromatin using these recombinant *S. pombe* octamers by salt step dialysis. Salt dialysis usually generates well assembled canonical nucleosomes but no extensive regular arrays (Figure 5, lanes 1–3). A classical nucleosome

spacing assay (Lusser and Kadonaga, 2004; Lusser *et al*, 2005) monitors if addition of a potential nucleosome spacing activity generates more extensive regular arrays in the presence of ATP. Indeed, incubation of salt dialysis chromatin with Hrp1 or Hrp3 generated much more extensive MNase ladders, but only in the presence of ATP (Figure 5, compare lanes 4–6 with 10–12 for Hrp1, and with 16–18 for Hrp3). The respective mock preparations were negative in this assay (Supplementary Figure 13) confirming that the spacing activity was due to Hrp1 and Hrp3, respectively, and not caused by co-purifying contaminants.

An alternative assay monitors both nucleosome assembly and spacing activity (Tsukiyama *et al*, 1999; Lusser and Kadonaga, 2004; Lusser *et al*, 2005). Here, the histone chaperone Nap1 is mixed with histones and DNA at physiological salt concentrations. Such chromatin is notoriously of low quality, i.e., rather susceptible to MNase digestion as histones are not always assembled into canonical nucleosomes (Nakagawa *et al*, 2001), and, importantly, are not extensively regularly spaced. This low quality chromatin allows to assay if a remodeling activity can generate regularly spaced nucleosomes in an ATP dependent manner. Also in this assay, both Hrp1 and Hrp3 generated more extensive MNase ladders in an ATP dependent way (Figure 6A) and the extent of the MNase ladder depended on the remodeler concentration (Figure 6B).

Note that the presence of ATP decreases the MNase digestion degree as seen by less trimming of the mononucleosomes (larger fragment size) and more abundant longer fragments (e.g., see Figures 5 and 6A, compare in each figure lanes 1–3 versus 4–6; see Supplementary Figure 12B for the different appearance of the same chromatin with different MNase digestion degrees). ATP has a bit higher affinity for Ca^{2+} than for Mg^{2+} ($\log K_D$ (HATP^{3-}) of -4.69 versus -4.55 , respectively (Martell and Smith, 1975)). Ca^{2+} is also sequestered by inorganic phosphate liberated during the remodeling reaction from creatine phosphate of the ATP regenerating system. So the presence of ATP together with the ATP regenerating system reduces the effective Ca^{2+} concentration and thereby the effective MNase activity. Therefore only the samples plus or minus ATP should be directly compared to each other, respectively. It is clear that Hrp1 and Hrp3 in the absence of ATP do not generate more extensive MNase ladders than salt dialysis or Nap1 alone (Figures 5 and 6A, compare in each figure lanes 7–9 and 13–15 versus 1–3), but do so only with ATP (Figures 5 and 6A, compare in each figure lanes 10–12 and 16–18 versus 4–6).

In summary, we give direct *in vitro* evidence using two different assay systems that both Hrp1 and Hrp3 have ATP-dependent nucleosome spacing activity. Interestingly, in both assays both remodeling enzymes generated the tight nucleosome repeat length observed for *S. pombe in vivo* (Lantermann *et al*, 2010; Givens *et al*, 2012).

Discussion

Here we demonstrate for the first time that the *S. pombe* CHD1-type remodeling enzymes Hrp1 and Hrp3 have nucleosome spacing activity *in vitro* and show correspondingly that they are redundantly necessary for the generation of TSS-aligned genic nucleosome arrays *in vivo*. Our observations very much parallel the findings in *S. cerevisiae* where Isw1,

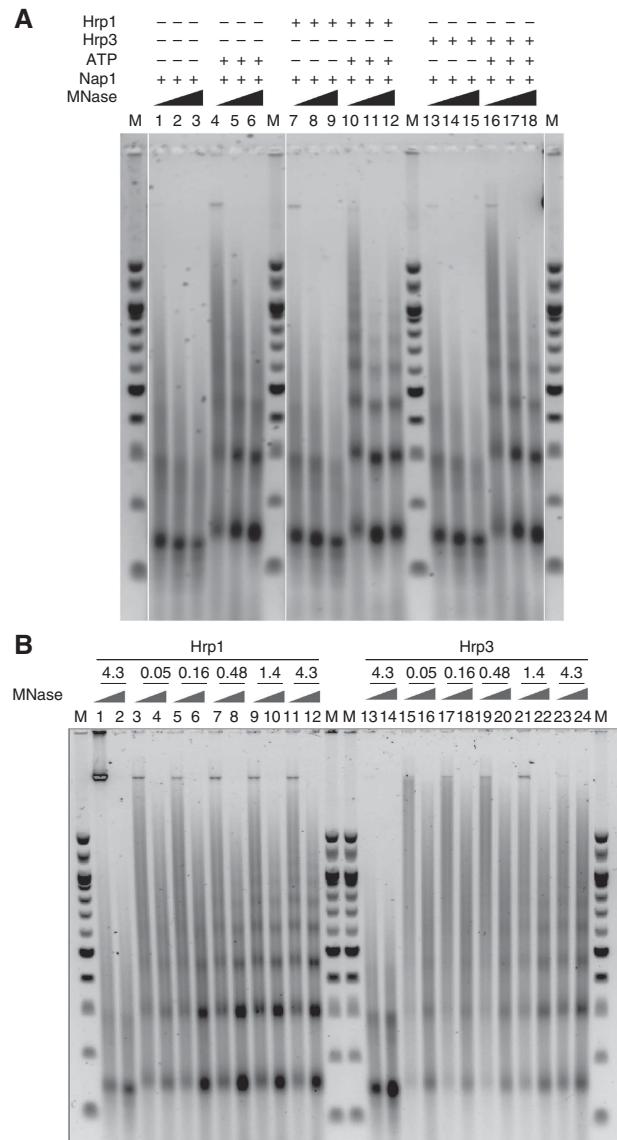


Figure 6 Hrp1 and Hrp3 show concentration- and ATP-dependent spacing activity in Nap1-assembly assay. **(A)** Phage λ DNA was mixed under physiological conditions with recombinant *S. pombe* histones, recombinant Nap1, purified Hrp1, Hrp3 and ATP as indicated on top of the lanes and digested with MNase (as in Figure 5). All samples were electrophoresed in the same gel, thin white lines mark horizontal rearrangement in Photoshop. **(B)** As panel **(A)** but with different Hrp1 and Hrp3 concentrations (in nM) as indicated. Samples in lanes 1, 2, 13 and 14 did not contain ATP. Lanes 'M' as in Figure 5.

Isw2 (Tsukiyama *et al*, 1999), and—by circumstantial evidence (Robinson and Schultz, 2003; Stockdale *et al*, 2006)—also Chd1 have nucleosome spacing activity *in vitro*, and where lack of Chd1 (Gkikopoulos *et al*, 2011; Lee *et al*, 2012) and even more so the combined absence of Isw1 and Chd1 (Gkikopoulos *et al*, 2011) also compromises genic arrays *in vivo*. In fact, our TSS-aligned composite nucleosome occupancy profile of the *S. pombe hrp1Δ hrp3Δ* double mutant is like a *déjà vu* of the respective profiles for the *isw1 chd1* double or *isw1 isw2 chd1* triple mutant in *S. cerevisiae* (Gkikopoulos *et al*, 2011). This argues that we are looking at the same functional defect in global

nucleosome organisation over coding regions in both distantly related yeasts. However, the machinery responsible for this function has undergone an evolutionary shift from using a combination of ISWI- and CHD1-type remodeling enzymes to using an expanded repertoire of CHD1-type remodelers, or the other way around. This may explain in part the long-standing conundrum of how *S. pombe* gets along without any ISWI-type remodeling enzymes (Flaus *et al*, 2006). Interestingly, at least two remodeling enzymes are redundantly involved in this function in both yeasts such that the effects in the respective single mutants are much smaller compared to the double or triple mutants.

Similar to *S. cerevisiae*, we did not find much of a global role of Swr1 or H2A.Z in nucleosome positioning in *S. pombe*, even though H2A.Z is enriched in the well positioned +1 nucleosome. The unusual nucleosome organisation with a more narrow NFR and rather prominent -1 to -3 nucleosomes upstream of the TSS at H2A.Z binding genes was not dependent on H2A.Z and Swr1 but may warrant further investigation. Our analysis of chromatin structure is carried out using unsynchronized *S. pombe* cultures consisting predominantly (>80%) of G2 cells. We showed that many H2A.Z binding genes are repressed in G2 cells and induced in other conditions such as during mitosis, meiosis or stress (Sadeghi *et al*, 2011). Maybe H2A.Z still plays a role in altering nucleosome organisation when these genes are induced and thereby facilitates their expression.

Much to our surprise, we did not see major defects in nucleosome positioning in the absence of RSC activity. We wonder if our restrictive conditions may have been too mild. They did induce a phenotype on cell growth and viability (Supplementary Figure 2) similar to the *sth1^{td}* phenotype in *S. cerevisiae* as used by Parnell *et al* (2008). However, in contrast to Parnell *et al* (2008), we did not test downregulation of new transcription or ablation of Snf21 on the protein level, which may reveal a different stringency of our *snf21-ts* phenotype in *S. pombe* compared to their *sth1^{td}* phenotype in *S. cerevisiae*. It remains to be clarified whether more complete ablation of Snf21 will reveal a role of RSC in nucleosome positioning in *S. pombe* after all.

Collectively, there were different roles of ISWI- and CHD1-type remodeling enzymes, and apparently of RSC, for global nucleosome organisation in both evolutionarily much diverged yeasts. This is a striking demonstration of the earlier notion that different mechanisms evolved to generate the same or similar chromatin architectures (Tsankov *et al*, 2010; Tsankov *et al*, 2011). So far the examples mainly pertained to different mechanisms of NFR generation, very recently also for NFRs at replication origins in three fission yeast species (Xu *et al*, 2012). To this we now add one more example, i.e., RSC has no major role in NFR formation in *S. pombe*. Importantly, we also found the first clear example of different mechanisms for the generation of TSS-aligned genic arrays.

Despite this interesting differential use of remodeling enzymes, both yeasts share an important mechanistic feature that was not highlighted so far. We noted that bulk MNase ladders were hardly compromised in the *hrp1Δ hrp3Δ* double mutant even though bulk MNase ladders mainly reflect genic regions due to the low percentage (about 5%) of intergenic regions, and even though genic arrays were severely impaired.

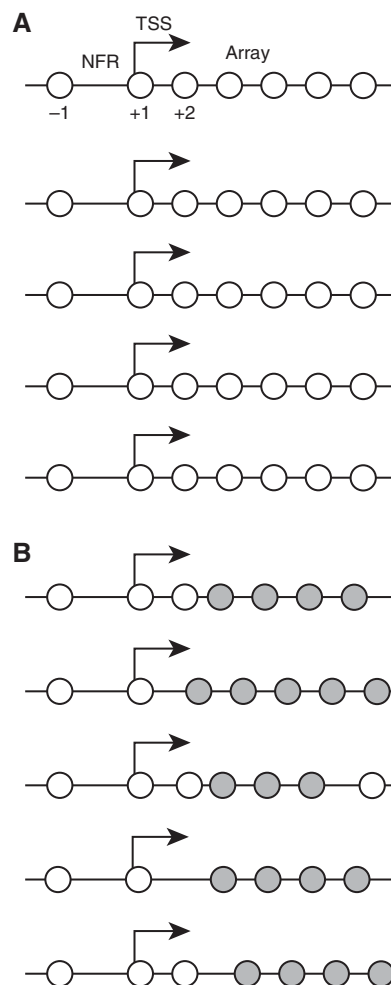


Figure 7 Schematic illustrating the difference between bulk spacing and TSS-aligned genic arrays. (A) TSS-aligned regular nucleosome arrays with the same spacing and register relative to the TSS for many different genes are the basis for the NFR-array nucleosome organization observed *in vivo*. (B) Regions of regularly spaced nucleosomes (grey circles) at different positions relative to the TSS for different genes (and maybe also per gene in different cells) will give rise to bulk MNase ladders but not to regular genic arrays in TSS-aligned nucleosome occupancy composite plots. Note that the positions of the NFR, the -1, +1, and less so the +2 nucleosomes may remain largely unchanged.

In our view this is similar to the *isw1 chd1* double or *isw1 isw2 chd1* triple mutant in *S. cerevisiae*. Even though we reproduced the defects seen by Gkikopoulos *et al* (2011), and even though there were more pronounced effects on signal intensity in *S. cerevisiae* than in *S. pombe*, we choose to underscore that bulk MNase ladders are still substantially detectable in all these mutants. This may seem contradictory to the impaired genic arrays, but note that MNase ladders monitor the average distance between nucleosomes regardless of their positions relative to genomic coordinates. In contrast, genic arrays require the combination of two criteria: regular nucleosome spacing and a fixed distance between TSS and array start (=TSS-alignment of arrays) (Figure 7). This is why the changed nucleosome organisation is detected if TSS-aligned nucleosome occupancy is plotted as an overlay of many genes, or in spectral analysis, which is linked to genomic coordinates, but not necessarily in bulk MNase ladders. Therefore, ISWI- and/or CHD1-type remodel-

ing enzymes, depending on the yeast species, are not essential to regularly space nucleosomes as such, but mainly to link regular nucleosomal arrays to the TSS in a fixed register for many different genes and for the same gene in different cells. Nonetheless, this fixed linkage may on average lead to longer contiguous regular arrays, which may explain the more or less pronounced defects in extents of bulk MNase ladders in some of these mutants. The Pugh group repeatedly suggested that the +1 nucleosome determines the TSS (Jiang and Pugh, 2009; Rhee and Pugh, 2012). Therefore it may amount to the same if the reference point for the ISWI- and/or CHD1-type remodeling enzymes is the TSS or the +1 nucleosome (or the NFR). The same authors argued very recently that various remodeling enzymes direct nucleosomes relative to ‘focal points’, i.e., to the TSS or also transcription termination sites (Yen *et al*, 2012), which fits with our notion that ISWI- and/or CHD1-type remodeling enzymes somehow link nucleosomal arrays to reference points. The main challenge for future studies will be to determine what anchors the +1 nucleosome and how remodeling enzymes exert directionality towards ‘focal points’.

We find it striking that even in the TSS-aligned composite plots for the respective double and triple mutants in both yeasts the +1 and +2 nucleosome positions (= peak positions) were unchanged, and only their occupancies (= peak areas) were affected. It seems that the nucleosome architecture in the immediate vicinity of the TSS is biologically very important. So far no viable mutant has been identified where this architecture was impaired suggesting an essential role. Further, even under conditions of decreased nucleosome density this architecture is actively maintained both *in vivo* (Celona *et al*, 2011; Gossett and Lieb, 2012) and *in vitro* (Zhang *et al*, 2011). Finally, the mutants with compromised genic arrays in both yeasts (see Gkikopoulos *et al* (2011) for *S. cerevisiae*) are relatively healthy and do not show widespread drastic changes in expression. Only 5.8% of all annotated transcripts changed more than 1.5 fold in sense expression and 7.2% showed cryptic antisense transcripts going up more than 1.5 fold in the *hrp1Δ hrp3Δ* mutant (Table I, Figure 2B). This mutant was not more sensitive to drugs challenging DNA repair (methylmethanesulfonate) or

DNA replication (hydroxyurea) (Supplementary Figure 14A and B), but did show some increased sensitivity to 200 and 300 μg/ml 6-azauracil, which reflects compromised transcription elongation (Supplementary Figure 14C). The latter fits well with the defects in chromatin structure over coding regions. Nonetheless, yeast cells appear to care a lot more about nucleosome positioning around the TSS, and can do rather well without regular genic arrays.

We show explicitly this rather loose correlation between impaired genic chromatin structure and expression changes for many genes (Figure 4C and Supplementary Figure 8E and F). Nonetheless, we may not have detected all changes in cryptic antisense transcription as some of the products may be degraded immediately by the RNA surveillance machinery. Also, our transcriptome analyses rely on the annotations for the wt, which is certainly a good approximation, but may not be totally accurate. The mutants may have changed transcription start and termination sites of annotated elements and the respective sites were not determined anew for the cryptic antisense transcripts. A genome-wide survey in *S. cerevisiae* identified at least 1000 genes with increased cryptic transcription in respective mutants (Cheung *et al*, 2008). The corresponding number is lacking for *S. pombe*, but it is likely that not every gene contains cryptic promoters, which may in turn explain why we detected much fewer increased cryptic antisense transcripts than chromatin changes. Importantly, the correlation is also not strict the other way around. The *set2Δ* mutant with increased cryptic transcription (Zofall *et al*, 2009) did not show defects in genic arrays (Supplementary Figure 10B and C). Collectively, this argues that impaired arrays can but need not cause changes in sense or cryptic antisense transcription and that the latter do not cause compromised arrays. In addition, changed levels of cryptic antisense transcription do not necessarily affect sense transcription in *S. pombe* (Supplementary Figure 9). Whether this contrasts with the respective regulation mechanisms suggested for *S. cerevisiae* (Xu *et al*, 2011) remains to be addressed specifically.

Hrp1 and Hrp3 were previously implicated in heterochromatin formation at centromeres and the mating type locus as well as in chromosome cohesion (Yoo *et al*, 2000; Jae *et al*, 2002; Walfridsson *et al*, 2005). At centromeres Hrp1 was

Table I Numbers of transcripts with changed expression levels

Strain comparison	>2 fold up	>1.5 fold up	Total up	>2 fold down	>1.5 fold down	Total down
<i>sense transcripts</i> ^a						
<i>hrp1Δ</i> versus wt	21 [10] (0.3%)	130 [59] (1.9%)	743 [233] (11%)	7 [2] (0.1%)	47 [9] (0.7%)	466 [46] (6.9%)
<i>hrp3Δ</i> versus wt	62 [37] (0.9%)	231 [119] (3.4%)	955 [282] (14.1%)	38 [15] (0.6%)	131 [43] (1.9%)	749 [130] (11.1%)
<i>hrp1Δ hrp3Δ</i> versus wt	96 [67] (1.4%)	251 [154] (3.7%)	783 [284] (11.6%)	28 [11] (0.4%)	142 [42] (2.1%)	665 [104] (9.9%)
<i>snf21-36(ts)</i> 34°C versus 25°C	111 [74] (1.6%)	395 [193] (5.9%)	2209 [470] (32.8%)	108 [30] (1.6%)	413 [98] (6.1%)	1964 [295] (29.1%)
<i>snf21-36(ts) sur1Δ</i> 34°C versus <i>snf21-36(ts)</i> 25°C	48 [36] (0.7%)	187 [102] (2.8%)	1977 [381] (29.3%)	54 [17] (0.8%)	306 [77] (4.5%)	1961 [361] (29.1%)
<i>pht1Δ sur1Δ</i> versus wt	435 [144] (6.5%)	1182 [375] (17.5%)	2120 [550] (31.4%)	252 [23] (3.7%)	761 [45] (11.3%)	1673 [110] (24.8%)
<i>cryptic antisense transcripts</i> ^b						
<i>hrp1Δ</i> versus wt	24 [2] (0.36%)	150 [40] (2.2%)	711 [379] (10.5%)	0 [3] (0%)	5 [14] (0.1%)	41 [132] (0.6%)
<i>hrp3Δ</i> versus wt	60 [21] (0.9%)	278 [74] (4.1%)	875 [401] (13.0%)	12 [6] (0.2%)	35 [29] (0.5%)	112 [214] (1.7%)
<i>hrp1Δ hrp3Δ</i> versus wt	125 [10] (1.9%)	457 [41] (6.8%)	1027 [355] (15.2%)	4 [30] (0.1%)	27 [95] (0.4%)	93 [202] (1.4%)

^aSense transcripts correspond to all 6742 annotated elements (2008 version) including ncRNAs that may be antisense to a coding RNA. The number of ncRNAs is given in square brackets. The percentage of all annotated elements is given in round brackets. Note that not all loci have proper TSS annotations, which is why numbers in this table are not the same as numbers for genes in TSS-aligned nucleosome occupancy composite plots.

^bCryptic antisense transcripts correspond to transcripts that are antisense to an annotated element, unless the antisense transcript overlaps with and shows a similar ($\pm 20\%$) change as an annotated element already scored as a sense transcript. The number of antisense transcripts filtered out according to the latter criterion is given in square brackets.

suggested to evict histone H3 in order to allow deposition of the centromere specific histone H3 variant Cnp1^{CENP-A} (Walfridsson *et al*, 2005). The function of Hrp1 at centromeres is linked to non-coding transcription (Choi *et al*, 2011). As our Nap1 *in vitro* assay monitors not only nucleosome spacing, but also nucleosome assembly (Nakagawa *et al*, 2001) and as both Hrp1 and Hrp3 were positive in this assay, Hrp1 may also directly assemble Cnp1^{CENP-A} at centromeres. This process could be linked to transcriptional elongation, just like the role of Hrp1 in generating nucleosome arrays in coding regions. The putative centromeric nucleosome assembly function of Hrp1 and Hrp3 will be explicitly addressed in a future study. In this regard it is interesting that Hrp3 co-purifies with histones (Supplementary Figure 12A and Supplementary Table I).

We reported both increased and decreased histone H3 density at both coding (ORF) and promoter regions (IGR) in *hrp1Δ* or *hrp3Δ* cells (Walfridsson *et al*, 2007). Especially at Hrp1 and Hrp3 targets in promoter regions there was more H3 binding. We did not observe such an effect in promoter regions in terms of MNase resistant nucleosome occupancy (Figure 4A and Supplementary Figure 7A). If anything, we saw decreased nucleosome occupancy over promoter and coding regions at Hrp1 and Hrp3 binding targets. This discrepancy may be due to the different assays used. Here we employ MNase-chip methodology, i.e., score only MNase resistant DNA. The earlier study used anti-H3-ChIP-chip, i.e., scored all histone H3-DNA interactions regardless of formation of canonical nucleosomes. There is also a technical difference between the microarray platforms used possibly explaining the poor agreement between the results. We used spotted microarrays for anti-H3-ChIP-chip containing one 400bp probe for each IGR and one 400bp ORF probe with a 3' bias (Wiren *et al*, 2005), and here we used tiling arrays with 20bp resolution. Another possible explanation is the formation of non-canonical nucleosome structures in the mutants. In *S. cerevisiae* it was shown that the absence of the histone chaperone Nap1 leads to increased formation of non-canonical nucleosomal particles (Andrews *et al*, 2010). We speculate that the absence of Hrp1 and/or Hrp3 has the same effect, which may translate into more DNA-bound H3 that can be detected by ChIP, but not by MNase digest.

It was argued for the case of *S. cerevisiae* that proper reassembly and positioning of nucleosomes in the wake of elongating RNA polymerase is important to prevent nonsense transcription from cryptic promoters (Kaplan *et al*, 2003; Cheung *et al*, 2008; Quan and Hartzog, 2010; Owen-Hughes and Gkikopoulos, 2012). Especially the roles of Chd1 and Isw1 in this context were recently recognized. Histone turnover over coding regions is increased in the budding yeast *chd1* or *isw1* single and even more so in the *chd1 isw1* double mutant, particularly in 3' ORF regions and at long genes (Radman-Livaja *et al*, 2012; Smolle *et al*, 2012). This is linked to changes in histone modifications over coding regions—e.g., hyperacetylation of histone H3 and H4, incorporation of histone H3 acetylated at lysine 56 (H3K56ac), less monoubiquitinated histone H2B (H2Bub) and a more 5' distribution of histone H3 methylated at lysine 36 (H3K36me) (Quan and Hartzog, 2010; Radman-Livaja *et al*, 2012; Lee *et al*, 2012; Smolle *et al*, 2012), and to increased cryptic

transcription (Cheung *et al*, 2008; Quan and Hartzog, 2010; Smolle *et al*, 2012), whereas expression of sense transcripts is only mildly affected (Tran *et al*, 2000; Gkikopoulos *et al*, 2011; Radman-Livaja *et al*, 2012; Lee *et al*, 2012). Our work highlights a similar mechanistic role for the two Chd1 homologues in *S. pombe*, Hrp1 and Hrp3, being involved in establishing proper nucleosome positioning over coding regions and preventing cryptic antisense transcription. Our work also directly demonstrates nucleosome spacing activity of these enzymes *in vitro*. Fission yeast and budding yeast are evolutionarily distinct (Forsburg, 1999; Heckman *et al*, 2001). If a function is conserved between these yeasts it is likely to be general in eukaryotes. Indeed, the effects of Chd1 on histone turnover (Radman-Livaja *et al*, 2012) and H2Bub levels (Lee *et al*, 2012) were explicitly demonstrated in fly and human cells, respectively. Chd1 plays an important regulatory role during cell differentiation of mouse embryonic stem cells (Gaspar-Maia *et al*, 2009). Thus, it is possible that suppression of cryptic antisense transcription by Chd1-type remodelers in coding regions is an important aspect of its function in mammalian development.

After submission of the revised version of our manuscript, a complementary study by Shim *et al* (2012) became available through advanced online publication. The overall conclusion is similar to ours in that Hrp3 was found to position nucleosomes over coding regions and to prevent non-coding transcription. However, the role of Hrp1 was missed. The nucleosome positioning defects in an *hrp1Δ* single mutant were found to be only slight, in agreement with our results (Figure 3A), and *hrp1Δ* cells were tested for transcriptional changes at only one locus, which was negative. In contrast, our genome-wide transcriptome analysis (Figure 2 and Table I) and the exacerbated nucleosome positioning defects in the *hrp1Δ hrp3Δ* double mutant compared to the *hrp3Δ* single mutant (Figure 3C) revealed that Hrp1 and Hrp3 are both involved in nucleosome positioning and suppression of cryptic transcription.

The increase in cryptic transcription in both fission and budding yeast mutants ultimately begs the question of what provides the window of opportunity for RNA polymerase to access cryptic promoters, which are presumably occluded by nucleosomes in wt cells. Are these nucleosomes destabilized at their wt positions, removed in *trans* (disassembled) or removed in *cis* (repositioned)? All three possibilities are not mutually exclusive and compatible with the observed increased histone turnover in budding yeast (Radman-Livaja *et al*, 2012; Smolle *et al*, 2012), which remains to be shown explicitly for fission yeast. Furthermore, all three modes would involve remodelers, which makes it especially attractive that specific remodeler types have now been identified in this context in both yeast species. Destabilization and disassembly of nucleosomes amounts to lower occupancy levels of canonical nucleosomes, which may be experimentally reflected in increased MNase sensitivity, while the third possibility would result in changed nucleosome positioning patterns. Apparently, there are different pathways involved as both the *set2Δ* and *hrp3Δ* mutants show increased cryptic transcription ((Zofall *et al*, 2009; Shim *et al*, 2012), Figure 2 and Table I) and increased histone turnover in the respective budding yeast mutants (Venkatesh *et al*, 2012; Smolle *et al*, 2012), but nucleosome positioning was only affected in *hrp3Δ* and not in *set2Δ* cells

Table II Yeast strains used in this study

Strain	Genotype	Source
<i>S. pombe</i>		
Hu0303	<i>h- 972</i>	
K240/Hu2261	<i>h- leu1-32</i>	Yamada <i>et al</i> (2008)
KYP176/Hu2262	<i>h- leu1-32 snf21-36(ts)</i>	Yamada <i>et al</i> (2008)
Hu2314	<i>h + snf21-36(ts) swr1D::ura4 + ura4D leu1-32</i>	This study
Hu2315	<i>h + snf21-36(ts) swr1D::ura4 + ura4D leu1- ade6 M216</i>	This study
Hu2239	<i>h- hrp1::ura4 ade6-M210 leu1-32 ura4-D18</i>	This study, <i>hrp1::ura4</i> allele from Jin <i>et al</i> (1998)
Hu0574/EJY322	<i>h + ade6-M216 leu1-32 ura4-D18 hrp3::leu2 +</i>	Jae <i>et al</i> (2002)
Hu0575/EJY321	<i>h- ade6-M210 leu1-32 ura4-D18 hrp3::leu2 +</i>	Jae <i>et al</i> (2002)
Hu0807	<i>h- hrp3:: leu2 + leu1-32</i>	Walfridsson <i>et al</i> (2007)
Hu2303	<i>h + hrp1::ura4 hrp3::leu2 + ade6-M210/6 leu1-32 ura4-D18</i>	This study
Hu2304	<i>h + hrp1::ura4 hrp3::leu2 + ade6-M210/6 leu1-32 ura4-D18</i>	This study
Hu1294	<i>h- mit1::KanMX6 leu1-32 ade6-210 ura4-DS/E</i>	H Bhuiyan
Hu1582	<i>h + set2::KanMX leu1-32</i>	Ekwall group
Hu2127	<i>htz1::KanMX swr1::ura4 ade6-M210/6 leu1-32 ura4D18</i>	This study
Hu2204	<i>h- hrp3::leu2 + leu1-32 hrp1-2xFLAG:KanMX</i>	This study
Hu2402	<i>h- hrp1::ura4, ade6-M210 leu1-32 ura4-D18 Hrp3-TAP:KanMX</i>	This study
<i>S. cerevisiae</i>		
W1588-4C	W303-1A but <i>RAD5</i>	Tsukiyama <i>et al</i> (1999)
YTT227	W1588-4C but <i>isw1::ADE2 isw2::LEU2 chd1::TRP1</i>	
BMA64	<i>MATα ura3-1 ade2-1 his3-11,5 trp1Δ leu2-3,112 can1-100</i>	Baudin <i>et al</i> (1993)
MP280 (= MP28)	BMA 64 but <i>isw1::URA3 chd1::kanMX isw2::TRP1</i>	Gkikopoulos <i>et al</i> (2011)

(Figure 3B and Supplementary Figure 10B and C). Shim *et al* (2012) report that chromatin from *hrp3 Δ* cells was significantly more sensitive to MNase and high salt washes. In contrast, in our hands, MNase ladders appeared not much changed in the *hrp3 Δ* and only slightly more so in the *hrp1 Δ hrp3 Δ* mutant (Supplementary Figure 11A). This discrepancy may be related to different MNase ladder appearances when using the same mutation in different *S. cerevisiae* strain backgrounds (Supplementary Figure 11B versus C). We caution that MNase ladders may appear different—both in ladder extent and even more so in signal intensity, which is difficult to normalize between samples—for many technical reasons even though the tested chromatin is the same or similar, while it is difficult to achieve unchanged MNase ladders for truly different chromatin if samples are treated in parallel. As mentioned above and noted by others (Radman-Livaja *et al*, 2012), we choose the view that MNase ladders are not much compromised upon lack of Chd1-type remodelers in both yeast species arguing against the possibility that global instability or substantial removal of nucleosomes are the main reason for providing access to cryptic promoters in these mutants. Instead, we propose that not only Chd1-type, but also other remodelers may re-establish canonical nucleosomes in the wake of RNA polymerase (maybe the same that are responsible for histone turnover), and that Chd1-type remodelers are specifically necessary to space nucleosomes in register to the TSS, consistent with their *in vitro* spacing activity. Nonetheless, lacking this specific spacing function may also translate into decreased nucleosome occupancy as irregular spacing over coding regions may increase nucleosome eviction by RNA polymerase (Engelholm *et al*, 2009). Indeed, our nucleosome occupancy profiles (Figure 3B and C, compare areas under the curves, which also reflect MNase sensitivity, but are also difficult to normalize between samples) may point to decreased nucleosome occupancy over coding regions in *hrp3 Δ* and *hrp1 Δ hrp3 Δ* cells. In summary, the effects on nucleosome occupancy appeared less robust

and dramatic than the effects on nucleosome positioning, which is why we highlight the mechanistic importance of the latter without dismissing the relevance of the former.

The study from Shim *et al* (2012) provides interesting additional data on the role of Hrp3 at centromeres. The *hrp3 Δ* mutant shows altered centromeric chromatin structure especially in the central core region where the centromeric CENP-A containing nucleosomes are localized (Shim *et al*, 2012). Here, we have not specifically addressed whether Hrp1 and Hrp3 cooperate also at centromeres. However, this is very likely given that Hrp1 is localized to the central core region where it is required for CENP-A localization, and in the light of the additive effects of *hrp1 Δ* and *hrp3 Δ* deletions with respect to chromosome segregation defects (Walfridsson *et al*, 2005). As mentioned above, it is conceivable that nucleosome disassembly and reassembly by Hrp1 and Hrp3 during non-coding transcription plays a role in maintaining proper CENP-A levels at centromeres.

Materials and methods

Yeast strains and media, spotting assays, viability assays and microscopy

Strains used in this study are given in Table II. For details on growth conditions, viability assays and microscopy see the Supplementary information.

S. pombe nucleosome occupancy measurements and processing of microarray data including spectral analysis

As in Lantermann *et al* (2009) and Lantermann *et al* (2010) but with the following modifications. As we observed inconsistency of fragment size after fragmentation of isolated mononucleosomal DNA with DNaseI prior to hybridization, purified DNA was always kept in conditions without EDTA. Therefore, DNA was resuspended in water instead of TE buffer after phenol extraction and ethanol precipitation of MNase digested chromatin and electrophoresed in EDTA-free Tris/Glycine gel. Mononucleosomal DNA fragments isolated from the gel were resuspended in water after isopropanol precipitation. Final fragment size distribution was always controlled using BioAnalyzer (Agilent Technologies) prior to microarray hybridization.

TSS annotations for composite plots and lists of convergent and tandem gene orientation were according to the TSS annotation in Lantermann *et al* (2010).

H3K56me binding data for *S. pombe* (Supplementary Figure 10C) were from Sinha *et al* (2010).

Bulk MNase ladder assay and MNase indirect end labeling

Done as in Lantermann *et al* (2009). For details see Supplementary information.

***S. cerevisiae* chromatin preparation and bulk MNase ladder assay**

Done as in Almer *et al* (1986); Svaren *et al* (1995).

RNA extraction

For RNA analysis, total RNA was extracted from mid-logarithmic phase cells using the hot-phenol method. Briefly, cells were harvested by centrifugation at RT, resuspended in TES (10 mM TrisHCl pH7.5, 10 mM EDTA and 0.5% SDS) and transferred to preheated acid phenol (65°C). After a 45 min shaking incubation at 65°C, RNA was isolated by phenol-chloroform extraction. For microarray analysis, RNA was treated according to the Affymetrix total RNA labelling protocol (<http://www.affymetrix.com>).

Reverse transcription with actinomycin D

RNA from strains Hu303, Hu2239, Hu0574, Hu2303, and Hu2304 was treated as described in Marvin *et al* (2011) with slight modifications (see Supplementary information).

Transcription analysis

Duplicate raw data from Affymetrix (.CEL format) were normalized with R (version 2.15.1 for iOS). Strains were as in Table II with Hu0574 as *hrp3Δ* mutant, and strains Hu2314/2315 and Hu2304/2305 as duplicates for the respective double mutants. All cel files were normalized together using quantile normalization using the preprocessCore package and data for each probe were assigned to *S. pombe* genome coordinates (2008 alignment). Data was visualized and analyzed with Podbat (Sadeghi *et al*, 2011) using the 2008 *S. pombe* genome annotation. To generate lists of up- and downregulated elements, elements for which the Signal to Noise Ratio (SNR), $(\text{average}(\text{condition1}) - \text{average}(\text{condition2})) / (\text{standard deviation}(\text{condition1}) + \text{standard deviation}(\text{condition2}))$ was below 1 were removed. A threshold for background signal was assigned as 1.5 times the mean wild type interelement linear signal level. Elements for which the linear signal is below this threshold for both genotypes in a comparison were also removed. Finally, an element A was not considered to show altered cryptic antisense transcription if its antisense strand A' overlapped an annotated element B, and if A' and B showed the same (+/-20%) alteration in transcription. The numbers of such cases where A' had a corresponding B are given in square brackets in the 'cryptic antisense transcription' part of Table I. Cryptic antisense versus sense scatterplots were generated using R (version 2.15.1 for iOS).

Purification of Hrp1-FLAG, Hrp3-TAP, and recombinant *S. pombe* histones and His-Nap1

C-terminally tagged Hrp1 and Hrp3 were affinity purified from 15 l cultures of Hu2204 and Hu2402, respectively. Harvested cells were frozen in liquid nitrogen, ground to fine powder (freezer mill 6870, Spex centriprep Ltd.), and S100 extracts were prepared for Hrp1-FLAG and Hrp3-TAP as described in Tsukiyama *et al* (1999) and Samuelsen *et al* (2003); Khorosjutina *et al* (2010), respectively. Hrp1-FLAG purification was modified as single step purification where Hrp1-FLAG was bound with M2 agarose beads (Sigma) and washed extensively with buffer containing 500 mM NaCl before elution with FLAG peptide at a final concentration of 1 mg/ml. For Hrp1-TAP purification IgG beads were washed with 300 mM salt followed by digestion with TEV protease. Eluted proteins were concentrated using Amicon concentrator of 50 000 Da cut off. Purified proteins were separated on 4–12% bis-tris denaturing gel in MOPS buffer and stained with either coomassie brilliant blue or Sypro ruby. Mock FLAG purifications were carried out in similar manner from two different strains Hu0807 and Hu2304 while Hu2304 was used for mock-TAP purification.

For cloning and purification of recombinant *S. pombe* histones and His-Nap1 see the Supplementary information.

Nap1 nucleosome assembly and spacing assay

Nucleosome assembly and spacing assay was carried out as described in Tsukiyama *et al* (1999) except that all buffer contained sodium salts. Briefly, 250 ng phage lambda DNA and 250 ng recombinant *S. pombe* histone octamers were added in the presence or absence of recombinant His-Nap1 (0.9 μg), ATP (3 mM ATP, 3 mM MgCl₂, 30 mM creatine phosphate, 1 ng/μl creatine kinase). Samples 'without ATP' also did not contain the extra 3 mM MgCl₂, but did contain creatine phosphate and creatine kinase, Hrp1 (4.3 nM, or as indicated) or Hrp3 (4.3 nM, or as indicated) and incubated for 4 h at 30°C. Temperature was lowered to 25°C, CaCl₂ was added to final concentration of 2 mM followed by MNase digestion for 5 min. Reaction was stopped by adding EDTA and SDS (25 mM and 0.5% w/v final concentrations, respectively) and treated overnight with 0.2 mg/ml proteinaseK at 42°C. DNA was ethanol precipitated with 1 mg/ml glycogen as carrier, electrophoresed in 1.7% agarose gel and stained with gel red (Sigma).

Nucleosome spacing assay using chromatin assembled by salt step dialysis

Nucleosomes were assembled on phage lambda DNA with recombinant *S. pombe* histone octamers at 1:1 mass ratio along with 0.1 mg/ml BSA by step salt dialysis against 10 mM Tris-Cl pH 7.5, 0.25 mM EDTA and salt concentrations of 1200, 750, 350 mM for 3 h at 4°C each. The last dialysis was against the same buffer with 50 mM salt and 2% v/v glycerol for 6 h or overnight. Assembled chromatin was incubated in the presence or absence of ATP, Hrp1, Hrp3, or mock-FLAG and mock-TAP preparations, digested by MNase and processed as described for the Nap1 assembly assay.

Trypsin Digest and Mass Spectrometry

According to standard techniques. For details see Supplementary information.

Accession codes

The microarray data from this publication have been submitted to the GEO database [<http://www.ncbi.nlm.nih.gov/geo/>] and assigned the accession number GSE41024. The mass spectrometry data for the Hrp1 and Hrp3 purifications have been deposited at ProteomeXchange [<http://www.proteomexchange.org/>] with the accession codes: PXD000031 and PXD000041, respectively. The mass spectrometry data for the Hrp3 purification are also given as Excel table in Supplementary Table I.

Supplementary data

Supplementary data are available at *The EMBO Journal* Online (<http://www.embojournal.org>).

Acknowledgements

We are grateful to Dr Tobias Straub for help with data analysis, to Dr Lars Israel and Dr Axel Imhof at the Zentrallabor für Proteinanalytik (ZfP, University of Munich) for prompt mass spectrometry analysis, to the Clinical Proteomics Mass Spectrometry at Karolinska University Hospital and Science for Life Laboratory for providing assistance in mass spectrometry and data analysis, to Dr Dietmar Martin and Kerstin Maier at the Affymetrix facility (Gene Center, University of Munich), and to Wenbo Dong for help with tagged Hrp3 expression. We thank Dr K Ohta, Dr K Takahashi and Dr M Yanagida for providing *S. pombe* strains, and Dr J Mellor and Dr T Tsukiyama for *S. cerevisiae* strains. Work in the Korber group was funded by the German Research Community (DFG, grant KO 2945/1-1) and by the Bavarian Ministry of Sciences, Research and the Arts in the framework of the Bavarian Molecular Biosystems Research Network. Research in the Ekwall laboratory is supported by grants from the Swedish Cancer Society, the Swedish Research Council (VR) and the Göran Gustafsson foundation for research in Natural Sciences and Medicine.

Author contributions: Julia P conducted all nucleosome mapping experiments including data analysis with help from Tobias Straub, the assays for *snf21-ts* phenotype, the spotting assays with

6-AU and HU, the MNase ladders in Supplementary Figure 11A and prepared figures. Jenna P constructed strains Hu2314/5 and Hu2303/4, and did all Affymetrix transcriptome experiments. Jenna P and JPS did the bioinformatical transcriptome data analysis and prepared figures. Jenna P performed the tetrad dissection analysis and spotting assay with MMS. AS generated strains Hu2127 and Hu2239 and prepared *S. pombe* histone expression vectors. PP and UN-A did all histone purification and octamer preparation. PP generated strains Hu2204 and Hu2402, purified

tagged proteins, did all *in vitro* assays and prepared figures. NK did the MNase ladders in Supplementary Figure 11B and C. OK prepared recombinant Nap1. KE and PK initiated and supervised the project and co-wrote the manuscript.

Conflict of interest

The authors declare that they have no conflict of interest.

References

- Alen C, Kent NA, Jones HS, O'Sullivan J, Aranda A, Proudfoot NJ (2002) A role for chromatin remodeling in transcriptional termination by RNA polymerase II. *Mol Cell* **10**: 1441–1452
- Almer A, Rudolph H, Hinnen A, Hörz W (1986) Removal of positioned nucleosomes from the yeast *PHO5* promoter upon *PHO5* induction releases additional upstream activating DNA elements. *EMBO J* **5**: 2689–2696
- Andrews AJ, Chen X, Zevin A, Stargell LA, Luger K (2010) The histone chaperone Nap1 promotes nucleosome assembly by eliminating nonnucleosomal histone DNA interactions. *Mol Cell* **37**: 834–842
- Badis G, Chan ET, van Bakel H, Pena-Castillo L, Tillio D, Tsui K, Carlson CD, Gossett AJ, Hasinoff MJ, Warren CL, Gebbia M, Talukder S, Yang A, Mnaimneh S, Terterov D, Coburn D, Li YA, Yeo ZX, Clarke ND, Lieb JD, Hughes TR et al (2008) A library of yeast transcription factor motifs reveals a widespread function for Rsc3 in targeting nucleosome exclusion at promoters. *Mol Cell* **32**: 878–887
- Bai L, Ondracka A, Cross FR (2011) Multiple Sequence-Specific Factors Generate the Nucleosome-Depleted Region on CLN2 Promoter. *Mol Cell* **42**: 465–476
- Baudin A, Ozier-Kalogeropoulos O, Denouel A, Lacroute F, Cullin C (1993) A simple and efficient method for direct gene deletion in *Saccharomyces cerevisiae*. *Nucleic Acids Res* **21**: 3329–3330
- Bell O, Tiwari VK, Thoma NH, Schubeler D (2011) Determinants and dynamics of genome accessibility. *Nat Rev Genet* **12**: 554–564
- Bonisch C, Hake SB (2012) Histone H2A variants in nucleosomes and chromatin: more or less stable? *Nucleic Acids Res*
- Brogaard K, Xi L, Wang JP, Widom J (2012) A map of nucleosome positions in yeast at base-pair resolution. *Nature* **486**: 496–501
- Buchanan L, Durand-Dubief M, Roguev A, Sakalar C, Wilhelm B, Stralfors A, Shevchenko A, Aasland R, Shevchenko A, Ekwall K, Francis SA (2009) The Schizosaccharomyces pombe JmjC-protein, Msc1, prevents H2A.Z localization in centromeric and subtelomeric chromatin domains. *PLoS Genet* **5**: e1000726
- Cairns BR, Lorch Y, Li Y, Zhang MC, Lacomis L, Erdjument-Bromage H, Tempst P, Du J, Laurent B, Kornberg RD (1996) RSC, an essential, abundant chromatin-remodeling complex. *Cell* **87**: 1249–1260
- Celona B, Weiner A, Di Felice F, Mancuso FM, Cesarini E, Rossi RL, Gregory L, Baban D, Rossetti G, Grianti P, Pagani M, Bonaldi T, Ragoussis J, Friedman N, Camilloni G, Bianchi ME, Agresti A (2011) Substantial histone reduction modulates genomewide nucleosomal occupancy and global transcriptional output. *PLoS Biol* **9**: e1001086
- Cheung V, Chua G, Batada NN, Landry CR, Michnick SW, Hughes TR, Winston F (2008) Chromatin- and transcription-related factors repress transcription from within coding regions throughout the *Saccharomyces cerevisiae* genome. *PLoS Biol* **6**: e277
- Choi ES, Stralfors A, Castillo AG, Durand-Dubief M, Ekwall K, Allshire RC (2011) Identification of noncoding transcripts from within CENP-A chromatin at fission yeast centromeres. *J Biol Chem* **286**: 23600–23607
- Clapier CR, Cairns BR (2009) The biology of chromatin remodeling complexes. *Annu Rev Biochem* **78**: 273–304
- Davey CA, Sargent DF, Luger K, Maeder AW, Richmond TJ (2002) Solvent mediated interactions in the structure of the nucleosome core particle at 1.9 Å resolution. *J Mol Biol* **319**: 1097–1113
- Ekwall K (2007) Epigenetic control of centromere behavior. *Annu Rev Genet* **41**: 63–81
- Engelholm M, de Jager M, Flaus A, Brenk R, van Noort J, Owen-Hughes T (2009) Nucleosomes can invade DNA territories occupied by their neighbors. *Nat Struct Mol Biol* **16**: 151–158
- Flaus A, Martin DM, Barton GJ, Owen-Hughes T (2006) Identification of multiple distinct Snf2 subfamilies with conserved structural motifs. *Nucleic Acids Res* **34**: 2887–2905
- Forsburg SL (1999) The best yeast? *Trends Genet* **15**: 340–344
- Fu Y, Sinha M, Peterson CL, Weng Z (2008) The insulator binding protein CTCF positions 20 nucleosomes around its binding sites across the human genome. *PLoS Genet* **4**: e1000138
- Gaspar-Maia A, Alajem A, Polesso F, Sridharan R, Mason MJ, Heidersbach A, Ramalho-Santos J, McManus MT, Plath K, Meshorer E, Ramalho-Santos M (2009) Chd1 regulates open chromatin and pluripotency of embryonic stem cells. *Nature* **460**: 863–868
- Gelbart ME, Bachman N, Delrow J, Boeke JD, Tsukiyama T (2005) Genome-wide identification of lsw2 chromatin-remodeling targets by localization of a catalytically inactive mutant. *Genes Dev* **19**: 942–954
- Givens RM, Lai WK, Rizzo JM, Bard JE, Mieczkowski PA, Leatherwood J, Huberman JA, Buck MJ (2012) Chromatin architectures at fission yeast transcriptional promoters and replication origins. *Nucleic Acids Res* **40**: 7176–7189
- Givens RM, Mesner LD, Hamlin JL, Buck MJ, Huberman JA (2011) Integrity of chromatin and replicating DNA in nuclei released from fission yeast by semi-automated grinding in liquid nitrogen. *BMC Res Notes* **4**: 499
- Gkikopoulos T, Schofield P, Singh V, Pinskaya M, Mellor J, Smolle M, Workman JL, Barton GJ, Owen-Hughes T (2011) A role for Snf2-related nucleosome-spacing enzymes in genome-wide nucleosome organization. *Science* **333**: 1758–1760
- Gossett AJ, Lieb JD (2012) In Vivo Effects of Histone H3 Depletion on Nucleosome Occupancy and Position in *Saccharomyces cerevisiae*. *PLoS Genet* **8**: e1002771
- Grewal SI (2010) RNAi-dependent formation of heterochromatin and its diverse functions. *Curr Opin Genet Dev* **20**: 134–141
- Halley JE, Kaplan T, Wang AY, Kobor MS, Rine J (2010) Roles for H2A.Z and its acetylation in GAL1 transcription and gene induction, but not GAL1-transcriptional memory. *PLoS Biol* **8**: e1000401
- Hartley PD, Madhani HD (2009) Mechanisms that specify promoter nucleosome location and identity. *Cell* **137**: 445–458
- Heckman DS, Geiser DM, Eidell BR, Stauffer RL, Kardos NL, Hedges SB (2001) Molecular evidence for the early colonization of land by fungi and plants. *Science* **293**: 1129–1133
- Henikoff S, Shilatifard A (2011) Histone modification: cause or cog? *Trends Genet* **27**: 389–396
- Iyer VR (2012) Nucleosome positioning: bringing order to the eukaryotic genome. *Trends Cell Biol* **22**: 250–256
- Iyer V, Struhl K (1995) Poly(dA:dT), a ubiquitous promoter element that stimulates transcription via its intrinsic DNA structure. *EMBO J* **14**: 2570–2579
- Jae YE, Kyu JY, Ae LM, Bjerling P, Bum KJ, Ekwall K, Hyun SR, Dai PS (2002) Hrp3, a chromodomain helicase/ATPase DNA binding protein, is required for heterochromatin silencing in fission yeast. *Biochem Biophys Res Commun* **295**: 970–974
- Jiang C, Pugh BF (2009) Nucleosome positioning and gene regulation: advances through genomics. *Nat Rev Genet* **10**: 161–172
- Jin YH, Yoo EJ, Jang YK, Kim SH, Kim MJ, Shim YS, Lee JS, Choi IS, Seong RH, Hong SH, Park SD (1998) Isolation and characterization of hrp1+, a new member of the SNF2/SWI2 gene family from the fission yeast *Schizosaccharomyces pombe*. *Mol Gen Genet* **257**: 319–329

- Kaplan CD, Laprade L, Winston F (2003) Transcription elongation factors repress transcription initiation from cryptic sites. *Science* **301**: 1096–1099
- Kaplan N, Moore IK, Fondufe-Mittendorf Y, Gossett AJ, Tillo D, Field Y, LeProust EM, Hughes TR, Lieb JD, Widom J, Segal E (2009) The DNA-encoded nucleosome organization of a eukaryotic genome. *Nature* **458**: 362–366
- Khorosjutina O, Wanrooij PH, Walfridsson J, Szilagy Z, Zhu X, Baraznenok V, Ekwall K, Gustafsson CM (2010) A chromatin-remodeling protein is a component of fission yeast mediator. *J Biol Chem* **285**: 29729–29737
- Kornberg RD (1974) Chromatin structure: a repeating unit of histones and DNA. *Science* **184**: 868
- Kornberg RD, Lorch Y (1999) Twenty-five years of the nucleosome, fundamental particle of the eukaryote chromosome. *Cell* **98**: 285–294
- Kornberg RD, Stryer L (1988) Statistical distributions of nucleosomes: nonrandom locations by a stochastic mechanism. *Nucl Acids Res* **16**: 6677–6690
- Kouzarides T (2007) Chromatin modifications and their function. *Cell* **128**: 693–705
- Lantermann A, Stralfors A, Fagerstrom-Billai F, Korber P, Ekwall K (2009) Genome-wide mapping of nucleosome positions in *Schizosaccharomyces pombe*. *Methods* **48**: 218–225
- Lantermann AB, Straub T, Stralfors A, Yuan GC, Ekwall K, Korber P (2010) *Schizosaccharomyces pombe* genome-wide nucleosome mapping reveals positioning mechanisms distinct from those of *Saccharomyces cerevisiae*. *Nat Struct Mol Biol* **17**: 251–257
- Lee JS, Garrett AS, Yen K, Takahashi YH, Hu D, Jackson J, Seidel C, Pugh BF, Shilatifard A (2012) Codependency of H2B monoubiquitination and nucleosome reassembly on Chd1. *Genes Dev* **26**: 914–919
- Lusser A, Kadonaga JT (2004) Strategies for the reconstitution of chromatin. *Nat Methods* **1**: 19–26
- Lusser A, Urwin DL, Kadonaga JT (2005) Distinct activities of CHD1 and ACF in ATP-dependent chromatin assembly. *Nat Struct Mol Biol* **12**: 160–166
- Martell AE, Smith RM (1975) *Critical stability constants*. Plenum Press
- Marvin MC, Clauder-Munster S, Walker SC, Sarkeshik A, Yates III JR, Steinmetz LM, Engelke DR (2011) Accumulation of noncoding RNA due to an RNase P defect in *Saccharomyces cerevisiae*. *RNA* **17**: 1441–1450
- Mason JA, Mellor J (1997) Isolation of nuclei for chromatin analysis in fission yeast. *Nucleic Acids Res* **25**: 4700–4701
- Mavrich TN, Jiang C, Ioshikhes IP, Li X, Venters BJ, Zanton SJ, Tomsho LP, Qi J, Glaser RL, Schuster SC, Gilmour DS, Albert I, Pugh BF (2008) Nucleosome organization in the *Drosophila* genome. *Nature* **453**: 358–362
- Mizuguchi G, Shen X, Landry J, Wu WH, Sen S, Wu C (2004) ATP-driven exchange of histone H2AZ variant catalyzed by SWR1 chromatin remodeling complex. *Science* **303**: 343–348
- Mobius W, Gerland U (2010) Quantitative test of the barrier nucleosome model for statistical positioning of nucleosomes up- and downstream of transcription start sites. *PLoS Comput Biol* **6**: e1000891
- Monahan BJ, Villen J, Marguerat S, Bahler J, Gygi SP, Winston F (2008) Fission yeast SWI/SNF and RSC complexes show compositional and functional differences from budding yeast. *Nat Struct Mol Biol* **15**: 873–880
- Nakagawa T, Bulger M, Muramatsu M, Ito T (2001) Multistep chromatin assembly on supercoiled plasmid DNA by nucleosome assembly protein-1 and ATP-utilizing chromatin assembly and remodeling factor. *J Biol Chem* **276**: 27384–27391
- Owen-Hughes T, Gkikopoulos T (2012) Making sense of transcribing chromatin. *Curr Opin Cell Biol* **24**: 296–304
- Parnell TJ, Huff JT, Cairns BR (2008) RSC regulates nucleosome positioning at Pol II genes and density at Pol III genes. *EMBO J* **27**: 100–110
- Perocchi F, Xu Z, Clauder-Munster S, Steinmetz LM (2007) Antisense artifacts in transcriptome microarray experiments are resolved by actinomycin D. *Nucleic Acids Res* **35**: e128
- Quan TK, Hartzog GA (2010) Histone H3K4 and K36 methylation, Chd1 and Rpd3S oppose the functions of *Saccharomyces cerevisiae* Spt4-Spt5 in transcription. *Genetics* **184**: 321–334
- Radman-Livaja M, Quan TK, Valenzuela L, Armstrong JA, van Welsem T, Kim T, Lee LJ, Buratowski S, van Leeuwen F, Rando OJ, Hartzog GA (2012) A key role for chd1 in histone h3 dynamics at the 3' ends of long genes in yeast. *PLoS Genet* **8**: e1002811
- Radman-Livaja M, Rando OJ (2010) Nucleosome positioning: how is it established, and why does it matter? *Dev Biol* **339**: 258–266
- Raisner RM, Hartley PD, Meneghini MD, Bao MZ, Liu CL, Schreiber SL, Rando OJ, Madhani HD (2005) Histone variant H2A.Z marks the 5' ends of both active and inactive genes in euchromatin. *Cell* **123**: 233–248
- Rhee HS, Pugh BF (2012) Genome-wide structure and organization of eukaryotic pre-initiation complexes. *Nature* **483**: 295–301
- Richmond TJ, Davey CA (2003) The structure of DNA in the nucleosome core. *Nature* **423**: 145–150
- Robinson KM, Schultz MC (2003) Replication-independent assembly of nucleosome arrays in a novel yeast chromatin reconstitution system involves antisilencing factor Asf1p and chromodomain protein Chd1p. *Mol Cell Biol* **23**: 7937–7946
- Sadeghi L, Bonilla C, Stralfors A, Ekwall K, Svensson JP (2011) Podbat: a novel genomic tool reveals Swr1-independent H2A.Z incorporation at gene coding sequences through epigenetic meta-analysis. *PLoS Comput Biol* **7**: e1002163
- Samuelson CO, Baraznenok V, Khorosjutina O, Spahr H, Kieselbach T, Holmberg S, Gustafsson CM (2003) TRAP230/ARC240 and TRAP240/ARC250 Mediator subunits are functionally conserved through evolution. *Proc Natl Acad Sci USA* **100**: 6422–6427
- Satchwell SC, Travers AA (1989) Asymmetry and polarity of nucleosomes in chicken erythrocyte chromatin. *EMBO J* **8**: 229–238
- Segal E, Fondufe-Mittendorf Y, Chen L, Thastrom A, Field Y, Moore IK, Wang JP, Widom J (2006) A genomic code for nucleosome positioning. *Nature* **442**: 772–778
- Segal E, Widom J (2009) Poly(dA:dT) tracts: major determinants of nucleosome organization. *Curr Opin Struct Biol* **19**: 65–71
- Sekinger EA, Moqtaderi Z, Struhl K (2005) Intrinsic histone-DNA interactions and low nucleosome density are important for preferential accessibility of promoter regions in yeast. *Mol Cell* **18**: 735–748
- Shim YS, Choi Y, Kang K, Cho K, Oh S, Lee J, Grewal SIS, Lee D (2012) Hrp3 controls nucleosome positioning to suppress non-coding transcription in eu- and heterochromatin. *EMBO J* (advance online publication, 18 September 2012; doi:10.1038/emboj.2012.267)
- Simic R, Lindstrom DL, Tran HG, Roinick KL, Costa PJ, Johnson AD, Hartzog GA, Arndt KM (2003) Chromatin remodeling protein Chd1 interacts with transcription elongation factors and localizes to transcribed genes. *EMBO J* **22**: 1846–1856
- Sinha I, Buchanan L, Ronnerblad M, Bonilla C, Durand-Dubief M, Shevchenko A, Grunstein M, Stewart AF, Ekwall K (2010) Genome-wide mapping of histone modifications and mass spectrometry reveal H4 acetylation bias and H3K36 methylation at gene promoters in fission yeast. *Epigenomics* **2**: 377–393
- Smolle M, Venkatesh S, Gogol MM, Li H, Zhang Y, Florens L, Washburn MP, Workman JL (2012) Chromatin remodelers Isw1 and Chd1 maintain chromatin structure during transcription by preventing histone exchange. *Nat Struct Mol Biol* **19**: 884–892
- Stockdale C, Flaus A, Ferreira H, Owen-Hughes T (2006) Analysis of nucleosome repositioning by yeast ISWI and Chd1 chromatin remodeling complexes. *J Biol Chem* **281**: 16279–16288
- Sugiyama T, Cam HP, Sugiyama R, Noma K, Zofall M, Kobayashi R, Grewal SI (2007) SHREC, an effector complex for heterochromatic transcriptional silencing. *Cell* **128**: 491–504
- Svaren J, Venter U, Hörz W (1995) *In vivo* analysis of nucleosome structure and transcription factor binding in *Saccharomyces cerevisiae*. *Methods in Mol Genet* **6**: 153–167
- Tirosh I, Sigal N, Barkai N (2010) Widespread remodeling of mid-coding sequence nucleosomes by Isw1. *Genome Biol* **11**: R49
- Tran HG, Steger DJ, Iyer VR, Johnson AD (2000) The chromatin domain protein chd1p from budding yeast is an ATP-dependent chromatin-modifying factor. *EMBO J* **19**: 2323–2331
- Tsankov A, Yanagisawa Y, Rhind N, Regev A, Rando OJ (2011) Evolutionary divergence of intrinsic and trans-regulated nucleosome positioning sequences reveals plastic rules for chromatin organization. *Genome Res* **21**: 1851–1862
- Tsankov AM, Thompson DA, Socha A, Regev A, Rando OJ (2010) The role of nucleosome positioning in the evolution of gene regulation. *PLoS Biol* **8**: e1000414

- Tsukiyama T, Palmer J, Landel CC, Shiloach J, Wu C (1999) Characterization of the imitation switch subfamily of ATP-dependent chromatin-remodeling factors in *Saccharomyces cerevisiae*. *Genes Dev* **13**: 686–697
- Valouev A, Ichikawa J, Tonthat T, Stuart J, Ranade S, Peckham H, Zeng K, Malek JA, Costa G, McKernan K, Sidow A, Fire A, Johnson SM (2008) A high-resolution, nucleosome position map of *C. elegans* reveals a lack of universal sequence-dictated positioning. *Genome Res* **18**: 1051–1063
- Valouev A, Johnson SM, Boyd SD, Smith CL, Fire AZ, Sidow A (2011) Determinants of nucleosome organization in primary human cells. *Nature* **474**: 516–520
- Venkatesh S, Smolle M, Li H, Gogol MM, Saint M, Kumar S, Natarajan K, Workman JL (2012) Set2 methylation of histone H3 lysine 36 suppresses histone exchange on transcribed genes. *Nature* **489**: 452–455
- Walfridsson J, Bjerling P, Thalen M, Yoo EJ, Park SD, Ekwall K (2005) The CHD remodeling factor Hrp1 stimulates CENP-A loading to centromeres. *Nucleic Acids Res* **33**: 2868–2879
- Walfridsson J, Khorosjutina O, Matikainen P, Gustafsson CM, Ekwall K (2007) A genome-wide role for CHD remodelling factors and Nap1 in nucleosome disassembly. *EMBO J* **26**: 2868–2879
- Whitehouse I, Rando OJ, Delrow J, Tsukiyama T (2007) Chromatin remodelling at promoters suppresses antisense transcription. *Nature* **450**: 1031–1035
- Wippo CJ, Israel L, Watanabe S, Hochheimer A, Peterson CL, Korber P (2011) The RSC chromatin remodelling enzyme has a unique role in directing the accurate positioning of nucleosomes. *EMBO J* **30**: 1277–1288
- Wiren M, Silverstein RA, Sinha I, Walfridsson J, Lee HM, Laurenson P, Pillus L, Robyr D, Grunstein M, Ekwall K (2005) Genomewide analysis of nucleosome density histone acetylation and HDAC function in fission yeast. *EMBO J* **24**: 2906–2918
- Xu J, Yanagisawa Y, Tsankov AM, Hart C, Aoki K, Kommasoyula N, Steinmann KE, Bochicchio J, Russ C, Regev A, Rando OJ, Nusbaum C, Niki H, Milos P, Weng Z, Rhind N (2012) Genome-wide identification and characterization of replication origins by deep sequencing. *Genome Biol* **13**: R27
- Xu Z, Wei W, Gagneur J, Clauder-Munster S, Smolik M, Huber W, Steinmetz LM (2011) Antisense expression increases gene expression variability and locus interdependency. *Mol Syst Biol* **7**: 468
- Yamada K, Hirota K, Mizuno K, Shibata T, Ohta K (2008) Essential roles of Snf21, a Swi2/Snf2 family chromatin remodeler, in fission yeast mitosis. *Genes Genet Syst* **83**: 361–372
- Yen K, Vinayachandran V, Batta K, Koerber RT, Pugh BF (2012) Genome-wide Nucleosome Specificity and Directionality of Chromatin Remodelers. *Cell* **149**: 1461–1473
- Yoo EJ, Jin YH, Jang YK, Bjerling P, Tabish M, Hong SH, Ekwall K, Park SD (2000) Fission yeast hrp1, a chromodomain ATPase, is required for proper chromosome segregation and its overexpression interferes with chromatin condensation. *Nucleic Acids Res* **28**: 2004–2011
- Yuan GC, Liu YJ, Dion MF, Slack MD, Wu LF, Altschuler SJ, Rando OJ (2005) Genome-scale identification of nucleosome positions in *S. cerevisiae*. *Science* **309**: 626–630
- Zhang Z, Wippo CJ, Wal M, Ward E, Korber P, Pugh BF (2011) A packing mechanism for nucleosome organization reconstituted across a eukaryotic genome. *Science* **332**: 977–980
- Zofall M, Fischer T, Zhang K, Zhou M, Cui B, Veenstra TD, Grewal SI (2009) Histone H2A.Z cooperates with RNAi and heterochromatin factors to suppress antisense RNAs. *Nature* **461**: 419–422